UNIVERSIDADE ESTADUAL DE CAMPINAS
Faculdade de Engenharia Mecânica

KEVIN BACHION CERIBELI

Fuel-Slurry Integrated Gasifier/Gas Turbine Process Using Municipal Solid Waste; Study on the Influence of Dry Solid Concentration in the Slurry on the Process Overall Power Efficiency

Processo Integrado de Gaseificador/Turbina a Gás Usando Resíduo Sólido Urbano como Combustível em Forma de Lama; Estudo da Influência do Teor de Sólido Seco na Lama na Eficiência Global do Processo

CAMPINAS
2018

KEVIN BACHION CERIBELI

Fuel-Slurry Integrated Gasifier/Gas Turbine Process Using Municipal Solid Waste; Study on the Influence of Dry Solid Concentration in the Slurry on the Process Overall Power Efficiency

Processo Integrado de Gaseificador/Turbina a Gás Usando Resíduo Sólido Urbano como Combustível em Forma de Lama; Estudo da Influência do Teor de Sólido Seco na Lama na Eficiência Global do Processo

Dissertation presented to the School of Mechanical Engineering of the University of Campinas in partial fulfillment of the requirements for the degree of Master in Mechanical Engineering, in the area of Energy.

Dissertação apresentada à Faculdade de Engenharia Mecânica da Universidade Estadual de Campinas como parte dos requisitos exigidos para a obtenção do título de Mestre em Engenharia Mecânica, na Área de Energia.

ESTE EXEMPLAR CORRESPONDE À VERSÃO FINAL DA DISSERTAÇÃO DEFENDIDA PELO ALUNO KEVIN BACHION CERIBELI, E ORIENTADA PELO PROF. DR MARCIO LUIZ DE SOUZA SANTOS

.....

ASSINATURA DO ORIENTADOR

CAMPINAS
2018

Agência(s) de fomento e nº(s) de processo(s): Não se aplica.

Ficha catalográfica
Universidade Estadual de Campinas
Biblioteca da Área de Engenharia e Arquitetura
Luciana Pietrosanto Milla - CRB 8/8129

C335f

Ceribeli, Kevin Bachion, 1991-
Fuel-slurry integrated gasifier/gas turbine process using municipal solid waste; study on the influence of dry solid concentration in the slurry on the process overall power efficiency / Kevin Bachion Ceribeli. – Campinas, SP : [s.n.], 2018.

Orientador: Marcio Luiz de Souza Santos.
Dissertação (mestrado) – Universidade Estadual de Campinas, Faculdade de Engenharia Mecânica.

1. Leito fluidizado. 2. Gaseificação. 3. Resíduos sólidos. I. Santos, Marcio Luiz de Souza, 1949-. II. Universidade Estadual de Campinas. Faculdade de Engenharia Mecânica. III. Título.

Informações para Biblioteca Digital

Título em outro idioma: Processo integrado de gaseificador/turbina a gás usando resíduo sólido urbano como combustível em forma de lama ; estudo da influência do teor de sólido seco na lama na eficiência global do processo
Palavras-chave em inglês:
Fluidized bed
Gasification
Municipal solid waste
Área de concentração: Térmica e Fluídos
Titulação: Mestre em Engenharia Mecânica
Banca examinadora:
Marcio Luiz de Souza Santos [Orientador]
Antonio Carlos Luz Lisbôa
Carlos Eduardo Keutenedjian Mady
Data de defesa: 06-02-2018
Programa de Pós-Graduação: Engenharia Mecânica

UNIVERSIDADE ESTADUAL DE CAMPINAS

FACULDADE DE ENGENHARIA MECÂNICA

COMISSÃO DE PÓS-GRADUAÇÃO EM ENGENHARIA MECÂNICA

DEPARTAMENTO DE ENERGIA

DISSERTAÇÃO DE MESTRADO ACADÊMICO

Fuel-Slurry Integrated Gasifier/Gas Turbine Process Using Municipal Solid Waste; Study on the Influence of Dry Solid Concentration in the Slurry on the Process Overall Power Efficiency

Processo Integrado de Gaseificador/Turbina a Gás Usando Resíduo Sólido Urbano como Combustível em Forma de Lama; Estudo da Influência do Teor de Sólido Seco na Lama na Eficiência Global do Processo

Autor: Kevin Bachion Ceribeli

Orientador: Prof. Dr. Marcio Luiz de Souza Santos

A Banca Examinadora composta pelos membros abaixo aprovou esta Dissertação/Tese:

Prof. Dr. Marcio Luiz de Souza Santos, Presidente
Instituição: FEM / UNICAMP

Prof. Dr. Carlos Eduardo Keutenedjian Mady
Instituição: FEM / UNICAMP

Prof. Dr. Dr. Antonio Carlos Luz Lisbôa
Instituição: FEQ / UNICAMP

A Ata da defesa com as respectivas assinaturas dos membros encontra-se no processo de vida acadêmica do aluno.

Campinas, 6 de fevereiro de 2018.

ACKNOWLEDGMENT

Special thanks to Professor Dr. Marcio Luiz de Souza Santos, for all the guidance patience, reliability, dedication, and opportunities.

I am very grateful to my beloved parents Rogério and Maria Cláudia, and to my dear siblings Harrison and Jessica, for all the care and incentive to always chase the best.

I am also very thankful to my loved fiancée Adriane, who has always been with me during the hardest moments. Certainly this path would be much harder if I haven't had her support.

My appreciation to professors and other contributors from the School of Mechanical Engineering of University of Campinas that allowed carrying my activities.

Success is 1% inspiration and 99% perspiration.

Thomas Edison

RESUMO

CERIBELI, Kevin Bachion, Processo Integrado de Gaseificador/Turbina a Gás Usando Resíduo Sólido Urbano como Combustível em Forma de Lama; Estudo da Influência do Teor de Sólido Seco na Lama na Eficiência Global do Processo, Faculdade de Engenharia Mecânica, Universidade Estadual de Campinas, Dissertação de Mestrado, (2018), 73 pp.

O presente trabalho pretende contribuir para os estudos de viabilidade teórica do conceito de Gaseificador/Turbina a Gás (FSIG/GT) integrados para geração de energia termelétrica aplicada ao caso de Resíduos Sólidos Urbanos (RSU). A lama é injetada por bombas comercialmente disponíveis em um secador pressurizado que opera sob a técnica de leito fluidizado borbulhante. Esse método evita os problemas comuns de alimentação de partículas em ambientes pressurizados. Após a secagem, o RSU é transportado para um gaseificador para produzir o gás combustível. O gás é limpo reduzindo-se a concentração e tamanhos de partículas para valores aceitáveis para injeção em turbinas a gás. Além disso, para atingir baixa concentração de componentes alcalinos, que podem causar erosão e corrosão nas lâminas da turbina de gás, a corrente de gás é arrefecida até valores abaixo das temperaturas de orvalho desses componentes alcalinos. O resfriamento fornece energia para a geração de vapor que impulsiona um ciclo baseado no ciclo Rankine. Em seguida, o gás é direcionado para um combustor e a corrente resultante a alta temperatura aciona turbina ou turbinas a gás. A exaustão dessas turbinas é usada para operar um ciclo Rankine secundário de recuperação de energia. O presente estudo aplica o software matemático (Simulador para Leitos Fluidizados e Moventes - CeSFaMB ©) para simular o secador e também o gaseificador, enquanto outro software (Simulador de Equipamentos e Processos Industriais - IPES ©) para simular processo global de geração de energia. Isso permite verificar o efeito do teor de sólidos secos na lama de RSU nas eficiências da 1ª e 2ª Lei da unidade global de geração de energia. Os resultados mostram um aumento praticamente linear dessas eficiências contra o aumento do teor de sólidos secos na lama. Também indica a possibilidade de melhorias substanciais no nível de eficiência global alcançado em trabalhos anteriores, atingindo agora valores superiores a 40%.

Palavras-chave: Leito Fluidizado, Gaseificação, Resíduo Sólido Urbano

ABSTRACT

CERIBELI, Kevin Bachion, Fuel-Slurry Integrated Gasifier/Gas Turbine Process Using Municipal Solid Waste; Study on the Influence of Dry Solid Concentration in the Slurry on the Process Overall Power Efficiency, School of Mechanical Engineering, University of Campinas, Master of Science Dissertation, (2018), 73 pp.

The present work intends to contribute to the theoretical feasibility studies of Fuel-Slurry Integrated Gasifier / Gas Turbine (FSIG / GT) concept for thermoelectric power generation applied to the case of Municipal Solid Waste (MSW). The slurry is injected by commercially available pumps into a pressurized dryer operating under the bubbling fluidized bed technique. Such a method avoids the commonly encountered problems of feeding particulates in pressurized environments. After drying, the MSW is carried to a gasifier to produce the fuel gas. The gas is cleaned by lowering its particle content and sizes to values acceptable for injection in gas turbines. Additionally, to reach low concentration of alkaline components, which might cause erosion and corrosion to gas turbine blades, the gas stream is cooled to values below the dew point temperatures of those alkaline components. The cooling provides energy for steam generation that drives a Rankine-based cycle. Then, the gas is directed to a combustor and the exiting hot stream turns gas turbine or turbines. The exhaust from those turbines is used to drive a secondary heat recovering Rankine-based cycle. The present study applies mathematical software (Comprehensive Simulator for Fluidized and Moving Beds - CeSFaMB©) to simulate the dryer as well the gasifier, while another software (Industrial Process and Equipment Simulator – IPES©) to simulate the whole power generation process. Those allow verifying the effect of dry solid content in the MSW slurry on the overall power unit 1st and 2nd Law efficiencies. The results show a practically linear increase of those efficiencies against the increase of dry solid content in the slurry. It also indicates the possibility of substantial improvements on the level of overall efficiency achieved in previous works, reaching now values higher than 40%.

Keywords: Fluidized Bed, Gasification, Municipal Solid Waste

LIST OF FIGURES

LIST OF TABLES

LIST OF SYMBOLS

a_j coefficient for representative formula of char. Subscripts indicate chemical element.

A area (m^2) or Ash (in chemical reactions)

b_j coefficients for representative formula of tar.

c specific heat at constant pressure (J kg^{-1} K^{-1})

d diameter (m)

D_j diffusivity of component "j" in the phase or media indicated afterwards (m^2 s^{-1})

f factor or fraction (dimensionless)

F mass flow (kg s^{-1})

g acceleration of gravity (m s^{-2})

G mass flux (kg m^{-2} s^{-1})

h enthalpy (J kg^{-1})

H height (m)

M mass (kg)

M_j molecular mass of component "j" (kmol/kg)

N_{Sh} Sherwood number (dimensionless)

p index for the particle geometry (0= planar, 1= cylindrical, 3= sphere)

p_j partial pressure of component "j" (Pa)

P pressure (Pa)

r radial coordinate (m)

r_i rate of reaction "i" (for homogeneous reactions: kg m^{-3} s^{-1}; for heterogeneous reactions: kg m^{-2} s^{-1})

R rate of mass or energy production (+) or consumption (-). Units depend of the usage. For instance, kg s^{-1} m^{-2} if due to heterogeneous reactions and kg s^{-1} m^{-3} if due to homogeneous reactions. For energy related parameters unit is W m^{-3}

S cross-sectional area (m^2). If no index, it indicates the cross-sectional area of reactor (m^2)

t time (s)

T temperature (K)

u velocity (m s^{-1})

U gas superficial velocity (m s^{-1}) or resistances to mass transfer (s m^{-2})

V volume (m^3)

x coordinate or distance (m)

x_j mole fraction of component "j" (dimensionless)

X elutriation parameter ($kg\ s^{-1}$)

y coordinate (m)

w_j mass fraction of component "j" (dimensionless)

z vertical coordinate (m)

z_D height of bed or dense region (m, measured from the surface of distributor)

z_F height of freeboard or lean region (m, measured from the surface of distributor)

GREEK LETTERS

α coefficient of heat transfer by convection ($W\ m^{-2}\ K^{-1}$)

ε void fraction (dimensionless)

ε' emissivity (dimensionless)

γ area of particles per volume of reactor or volume of indicated phase as index (m^2 / m^3)

γ_B area of bubbles per volume of reactor (m^2 / m^3)

Φ Thiele modulus

λ thermal conductivity ($W\ m^{-1}\ K^{-1}$)

Λ conversion fraction (dimensionless)

μ viscosity ($kg\ m^{-1}\ s^{-1}$)

ν_{ij} stoichiometry coefficient of component "j" in reaction "i"

ρ density or concentration ($kg\ m^{-3}$)

ρ_p apparent density of particle ($kg\ m^{-3}$)

ρ_j mass basis concentration of component "j" ($kg\ m^{-3}$) (in some situations the component "j" can be indicated by its formula)

σ Stefan-Boltzmann constant ($W\ m^{-2}\ K^{-4}$)

ψ mass transfer coefficient (s^{-1}: if between two gas phases; $kmol\ m^{-2}\ s^{-1}$: if between gas and solid)

SUBSCRIPTS

a general parameter or at the nucleus-outer-shell interface

A shell or residual layer

B	bubble
C	convection contribution. In some obvious situations, it would represent Carbon.
cond	conduction contribution
d	related to drying or dry basis
D	at or from the bed or dense region
E	emulsion
eq	equilibrium condition
F	at the freeboard or lean region
G	gas phase
h	transfer of energy due to mass transfer
H	related to the circulation of particles in a fluidized bed. In some obvious situations, it would represent Hydrogen.
hom	related to homogeneous (or gas-gas) reactions
het	related to heterogeneous (or gas-solid) reactions
i	reaction "i".
I	as at the feeding point
j	chemical component
l	level within the particle size distribution
L	at the leaving point or condition
m	physical phase (carbonaceous solid, m=1; limestone or dolomite, m=2; inert solid, m=3; gas, m=4)
M	mass generation or transfer
min	minimum condition
mf	minimum fluidization condition
N	nucleus or core. In some obvious situations, it would represent Nitrogen.
O	at or referred to external or outside surface. In some obvious situations, it would represent oxygen.
P	particle. If no other indication, property of particle is related to apparent value
P	at constant pressure
Q	related to chemical reactions
R	related to radiative heat transfer
S	solid phase or particles. If indicated for a property, such as density, it means apparent particle density. In some obvious situations, it would represent Sulphur.

T	terminal value or referred to tubes
tar	tar
U	unreacted-core model
v	related to devolatilization
V	volatile
W	wall
X	exposed-core model or related to elutriation
Y	related to entrainment of particles
z	related to axial or vertical direction
∞	at the gas phase far from the particle surface

SUPERSCRIPTS

~	in molar basis
‘	number fraction
“	area fraction
“‘	volume fraction

SUMMARY

1 INTRODUCTION

With the expansion of cities' population, the problem of Municipal Solid Waste (MSW) discard increases. On the other hand, sources of sustainable or renewable power generation should be explored.

The present study analyzes the theoretical feasibility of thermoelectric power generation based on pressurized gasifiers consuming MSW as fuel. It is mixed with water to form a slurry to be fed into the process. This process has been called Fuel-Slurry Integrated Gasification/Gas Turbine (FSIG/GT). The main objective is to verify the influence of the water content in the feeding slurry on the process overall efficiency. This might lead to information on how to improve the efficiency level arrived in previous studies on FSIG/GT.

1.1 BRAZILIAN ENERGY MATRIX

Energy matrix encompasses all the available energy to be generated, distributed and consumed in a country or region.

Brazil has one of the most renewable electric energy generation matrix in the industrialized world, with 75.5% coming from sources like hydro, biomass, wind, and solar power. In 2015, hydroelectric plants were responsible for the generation of 64.0% of the electricity of the country and biomass for 8.0%. In contrast, the world average energy matrix was composed by 24.1% of renewable sources, dropping to 23.1% in the countries of OCDE (Organization for the Cooperation and Economic Development) [1, 2].

The benefits of a renewable energy matrix are translated into reduced pollutant emissions, as well sustainable growth of energy offer. Data from 2016 shows that Brazil released 1.56 Mg of carbon dioxide per ton of oil equivalent (toe), while this indicator was 2.35 worldwide. In 2013, China and USA were responsible for 43.9% of world emissions, with 14.14 Mg CO2/toe. In the same year, the total emissions were accounted in 32.19 Mg CO2/toe [1].

Figure 1 illustrates the Brazilian electric matrix in 2015. It is noticeable that the hydroelectric generation is significantly higher than the other sources. It is also important to stress that biomass sources are the second most important. Among the biomass used for

purposes of electric power generation, are firewood, sugar cane bagasse, rice peels, black-liquor and municipal waste [2].

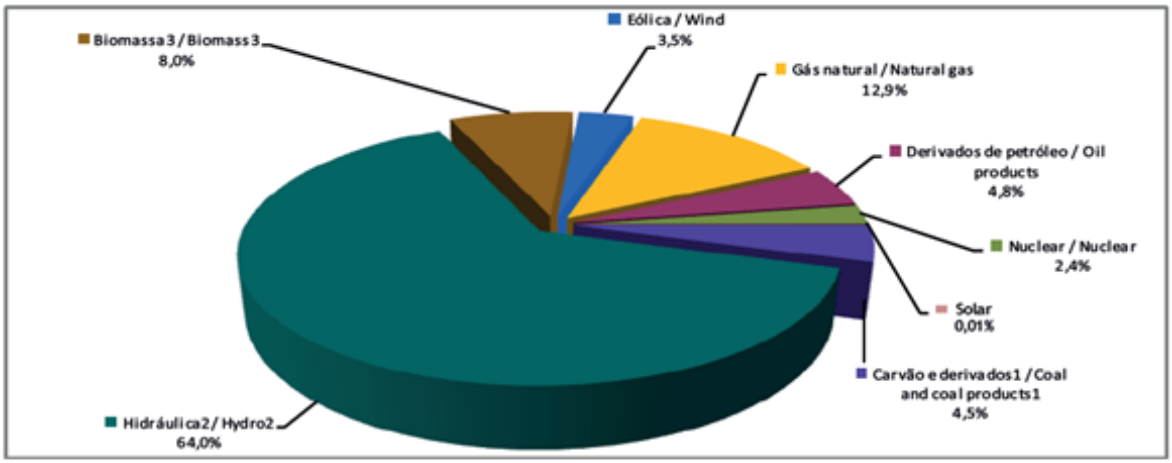

Notas/ *Notes*:

[1] Inclui gás de coqueria/ *Includes coke oven gas*

[2] Inclui importação de eletricidade/ *Includes electricity imports*

[3] Inclui lenha, bagaço de cana, lixívia e outras recuperações/ *Includes firewood, sugarcane bagasse, black-liquor and other primary sources*

Fonte/ *Source*: EPE

Figure 1. *Brazilian electric matrix, corresponding to 2015*

Based on researches from the Secretary of Planning and Energy Development, which assumes the Brazilian economy growing at 3.2% per year (world average value settled 3.8%), the Ministry of Mines and Energy created the Decennial Energy Expansion Plan (PDE). It envisages projections for the increase on installed capacity per generation source for the next years, and those are presented in Table 1 [3].

According to PDE, around R$ 1.4 trillion should be invested in the infrastructure of energy generation until 2024, with a 26.7% slice to the segment of electric power production, 70.6% to oil and natural gas, and 2.6%, to liquid biofuels [3]. Additionally, until 2024, that investment plan intends to increase the share of biomass and wind from 8.3% to 8.7%, and 3.7% to 11.6%, respectively. That is illustrated in Figure 2.

Table 1. *Evolution of installed capacity per generation source*

SOURCE	2014 (e)	2015	2016	2017	2018	2019	2020	2021	2022	2023	2024
						MW					
RENEWABLE	**111.269**	**118.380**	**127.866**	**135.486**	**142.972**	**145.177**	**145.560**	**151.554**	**158.102**	**165.460**	**173.417**
HYDRO (a)	82.789	86.540	92.152	96.587	101.354	102.040	102.115	103.549	105.137	107.335	109.972
IMPORT (b)	7.000	7.000	7.000	7.000	7.000	7.000	7.000	7.000	7.000	7.000	7.000
BIOMASS + WIND + SMALL HYDROPWER PLANT + SOLAR	21.480	24.840	28.714	31.899	34.618	36.137	36.445	41.005	45.965	51.125	56.445
NON RENEWABLE (c)	**21.609**	**21.913**	**22.082**	**22.092**	**22.493**	**26.714**	**28.230**	**29.430**	**30.630**	**31.830**	**33.030**
URANIUM	1.990	1.990	1.990	1.990	1.990	3.395	3.395	3.395	3.395	3.395	3.395
NATURAL GAS	11.043	11.317	11.486	12.026	12.427	14.903	16.419	17.619	18.819	20.019	21.219
COAL	3.064	3.064	3.064	3.064	3.064	3.404	3.404	3.404	3.404	3.404	3.404
FUEL OIL (d)	3.586	3.586	3.586	3.201	3.201	3.201	3.201	3.201	3.201	3.201	3.201
DIESEL OIL	1.239	1.269	1.269	1.124	1.124	1.124	1.124	1.124	1.124	1.124	1.124
PROCESS GAS	687	687	687	687	687	687	687	687	687	687	687
TOTAL	**132.878**	**140.293**	**149.948**	**157.578**	**165.465**	**171.891**	**173.790**	**180.984**	**188.732**	**197.290**	**206.447**
						Relative Participation (%)					
RENEWABLE	**83,7%**	**84,4%**	**85,3%**	**86,0%**	**86,4%**	**84,5%**	**83,8%**	**83,7%**	**83,7%**	**83,8%**	**84,0%**
HYDRO	67,6%	66,7%	66,1%	65,7%	65,5%	63,4%	62,8%	61,0%	59,3%	57,9%	56,7%
OTHERS	16,2%	17,7%	19,1%	20,2%	20,9%	21,0%	21,0%	22,7%	24,4%	26,0%	27,3%
NON RENEWABLE	**16,3%**	**15,6%**	**14,7%**	**14,0%**	**13,6%**	**15,5%**	**16,2%**	**16,3%**	**16,3%**	**16,2%**	**16,0%**
URANIUM	1,5%	1,4%	1,3%	1,3%	1,2%	2,0%	2,0%	1,9%	1,8%	1,7%	1,6%
OTHERS	14,8%	14,2%	14,7%	14,1%	13,4%	12,5%	12,5%	13,0%	13,4%	13,7%	14,5%
TOTAL	**100,0%**	**100,0%**	**100,0%**	**100,0%**	**100,0%**	**100,0%**	**100,0%**	**100,0%**	**100,0%**	**100,0%**	**100,0%**

Notes: (a) The values in the table indicate the installed power in December of each year, considering the hydroelectric power plants (HPP) motorization
(b) Estimate of the importation of HPP Itaipu not consumed b y the Paraguayan electrical system
(c) It doesn't consider self-production, which, for energy studies, is represented as charge reduction
(d) Values of installed capacity in December 2014, including the plants already in commercial operation in the isolated systems, with interconnection forecast within the horizon of the study
(e) Accounts for the plants that will be decomissioned over the period due to the interconnection of isoloated systems

Source: EPE

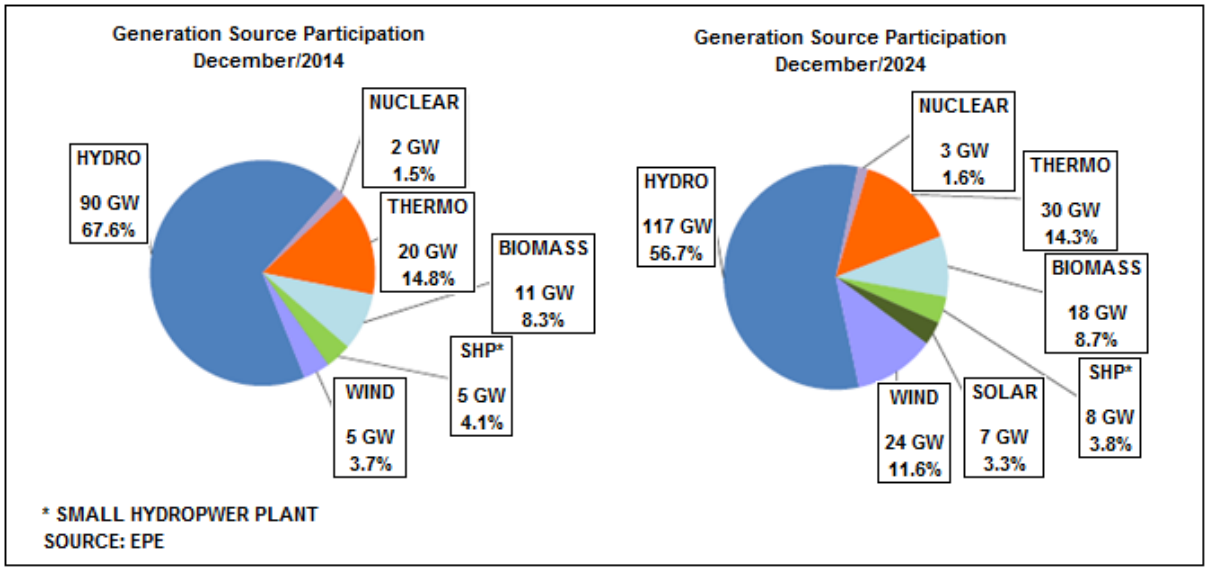

Figure 2. *Evolution of installed capacity per generation source*

Brazilian municipalities, such as São Paulo and Rio de Janeiro, respectively collect around 12,500 and 10,000 tons of MSW daily [4]. A fraction of those is recycled, leaving around 80% available for power generation. For the sake of an example, considering the Low Heating Value (LHV) of 10.17 MJ/kg (dry basis) – which was determined to the city of São Paulo elsewhere [5] - the power generation potential of that city can reach near 350 MW.

2 OBJECTIVE

Starting from a previous work [42], the objective of the present study is to investigate the influence of dry solid content in the water-MSW slurry on the efficiency of Fuel-Slurry Integrated Gasifier/Gas Turbine (FSIG/GT) power generation process consuming that slurry.

The basic concept of that power generation process is shown in Figure 3.

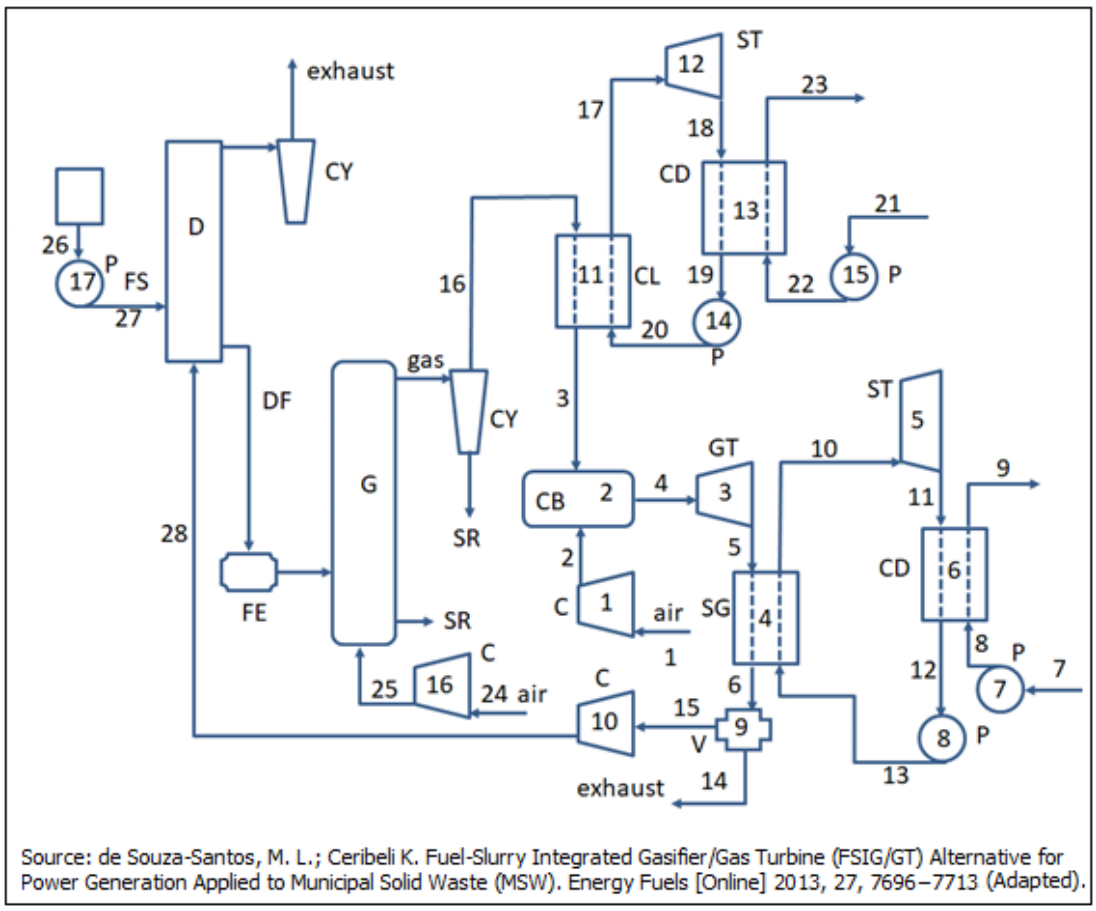

Source: de Souza-Santos, M. L.; Ceribeli K. Fuel-Slurry Integrated Gasifier/Gas Turbine (FSIG/GT) Alternative for Power Generation Applied to Municipal Solid Waste (MSW). Energy Fuels [Online] 2013, 27, 7696−7713 (Adapted).

Figure 3. *Configuration of the proposed FSIG/GT process*

C = Compressor, CB = Combustor, CD = Condenser, CL = Cleaning system, CY = Cyclones and Filters, D = Dryer, DF = Dried fuel, FE = Screw feeding, FS = Fuel-slurry pumping, G = Gasifier, GT = Gas turbine, SG = Steam generator, SR = Solid residue, ST = Steam turbine, P = Pump, V = Valve or Splitter.

According to that, water and wet MSW are mixed in order to form a slurry, which is pumped into a pressurized fluidized bed dryer. Since the dryer and gasifier operate at similar pressures, the dry fuel can be fed into the gasifier using simple rotary valves combined with Archimedes' screws. The fuel gas extracted from the gasifier is then cooled to temperatures below the dew-point of alkaline species, before entering the gas turbine. This operation is paramount to avoid alkaline species inside the gas turbine, which would cause erosion and corrosion of its blades [6-8]. Additionally, two energy-recovering cycles are coupled to the main process, in order to increase the overall efficiency of the entire process.

3 LITERATURE SURVEY

Application of rational and environmentally sound management of MSW is critical to achieve sustainable living conditions. Consequently, proper treatment and use of that residue for power generation remains among the most urgent problems of medium to large cities [9].

Currently, landfilling is the most common MSW disposing procedure [10]. For instance, in 2008, nearly 13 million tons of waste were generated by Canadian households and, from that, more than 8.5 million tons were disposed of in landfills or through incineration. The remaining 4.4 million tons were diverted for recycling, reuse, or composting. Paper fibers and organic materials represent the largest proportion of household material that is recycled and composted [11].

Although the widespread use of landfilling for waste disposal, it also brings several disadvantages. Among them the release of methane to the atmosphere, due to fermentation of biodegradable waste. That gas contributes to global warming, not to mention raises the potential for fires and explosions. In addition, rain water percolates through the landfill and dangerous pollutants might contaminate the underground water. Other impacts include the use of land and the retention of carbon in the landfill for long periods, with a fraction returning to the atmosphere as carbon dioxide. In addition, finding landfilling areas is progressively difficult, forcing increasing expenses in transportation of MSW to those areas [12].

On the other hand, open-air incineration brings even greater negative consequences than landfilling with the release of harmful pollutants such as NO_x, SO_2, HCl, fine particulates, dioxins, as well as carbon dioxide. Moreover, fly ash and residues from air pollution control systems require stabilization and disposal as hazardous waste. Proper combustion in power plants can eliminate many of the problems associated to open-air incineration as well allow energy recovery. As benefits, the generated power can replace a fraction of the produced by burning fossil fuels, thus bringing overall savings in carbon dioxide emissions. Additionally, the generated ash may be used as a secondary aggregate and recovered metals can be recycled [12]. Moreover, other modern alternatives can be applied to recover energy from MSW, such as refuse-derived fuel (RDF) production, mechanical-biological treatment, gasification and anaerobic digestion.

For these reasons, it is necessary to consider alternative municipal solid waste management strategies.

Unlike landfilling, composting reduces methane production from aerobic degradation of organic waste. Additionally, this method brings benefits because composites can be used as soil improvers and replace, to some extent, the use of fertilizers and peat, which have negative environmental impacts. Besides, composites can sequester carbon, thus increasing the stored soil organic matter and improving its fertility as well, allowing for decreases in the frequency of irrigation and lowering soil erosion rates. However, despite these advantages, careful control of the composting process should be set to avoid bio aerosols [12].

Mechanical-biological treatments reduce the volume of waste and therefore the area occupied by the landfill per mass of generated MSW and brings advantages as reduction of methane from aerobic degradation of treated organic waste in landfills. It also increases the recovering of materials for recycling and energy recovery [12]. However, the method still leads to most of the above-mentioned problems of landfilling.

As seen, all above mentioned methods have many negative points.

Aware of those difficulties, several Canadian municipalities have initiated or already developed successful recycling programs to reduce the amount of waste that goes to landfills [9]. Recycling, which has significantly increased in Canada, has led to energy saving because, usually, less energy is required to manufacture products from recycled feedstock than from original mineral or fossil resources. In this process, emissions of greenhouse gases and other pollutants are reduced as well. This method also prolongs reserves of finite resources (e.g. metal ores), contributing to the sustainable use of resources, and avoids impacts associated with extraction of virgin feedstock (e.g. quarrying of ores and sand, and felling of old growth forest to produce wood for paper) [12].

A headmost scenario can be observed in South Korea. It currently recycles 57% of household waste and sends 26% to landfills. The remaining 17% is fed into boilers and the generated steam used for heating. From the perspective of sustainable waste management, the priority is placed on the reduction of waste generation followed by recycling, both of which are highly beneficial in terms of greenhouse gas emissions reduction by saving resources otherwise required for manufacturing new products. Nonetheless, some wastes are not suitable for recycling and, for the non-recyclable fractions, an energy recovery method becomes important because it can reduce the use of fossil fuels. At the same time, it can also minimize the environmental and health problems of waste disposal applying the landfill alternative [13].

The Brazilian scenario related to MSW management needs urgent improvements. By 2015, about 60% of the collected MSW was sent to landfills, and almost 30% was conveyed to dumps, only the remaining found more appropriate destination, such as recycling [14].

Some environmental impacts of the main waste management options are summarized elsewhere [12].

Historically, several drawbacks were encountered in the development of processes using MSW as fuel for power generation. Among them, low efficiencies when compared with processes consuming more traditional fuels such as coals. That is mainly due to MSW's relatively high moisture content, low average heating value, and the challenges to comply with low pollutant emission standards [9-20].

Since the introduction of Coal Integrated Gasification/Gas Turbine (CIG/GT) and its biomass equivalent (BIG/GT) processes [21-29], most of their main technical obstacles have been overcome. For instance, the removal of tar [30, 32] from the produced gas as well lowering particle content and sizes and alkaline species concentrations in the produced gas in order to meet acceptable levels for injection into commercial turbines [30-35].

However, another important technical barrier, represented by the difficulty of feeding solid particulate fuels into pressurized vessels, remains. Usually, that feeding is accomplished by cascade or sequential systems, composed of two or more levels of pressurized lock hoppers [36, 37]. A scheme of the system is shown in Figure 4. The particulate fuel is fed at the top hopper. The pressure increases from a hopper to the following below, and that difference is not enough to cause particle densification when passing from one to the other. The last hopper drops the solid fuel on an Archimedes screw that feeds the fuel into the pressurized reactor. On the other hand, such operations involve high operational costs due to the use of cool inert gas to avoid fuel ignition or pyrolysis before it reaches the reactor. Furthermore, the mentioned alternative faces operational difficulties when handling fibrous fuels because neighboring particles tend to entangle, thus jeopardizing or even blocking the flow of material to the valve immediately below.

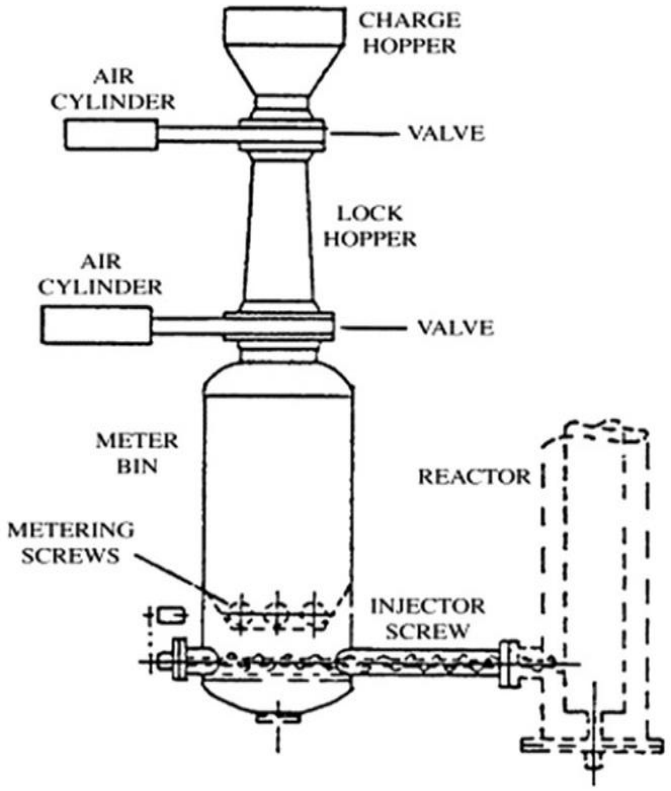

Figure 4. *Sequential lock-hopper feeding (Source: Dai, J.; Cui, H.; Grace, J. R. Biomass feeding for thermochemical reactors. Progress in Energy and Combustion Science [Online] 2012, 38 (5), 716-736)*

An alternative to circumvent that problem is to inject the fuel as a slurry into the pressurized reactor, using commercially available slurry pumps. This method has been applied for a long time [21] and greatly simplifies the feeding process and, very likely, decreases the capital, operational, and maintenance costs when compared with methods based on cascade systems of hoppers. Studies were developed exploring the option but mostly employing boilers [21, 38-41], because the vaporization of the fuel original moisture, added to the water to prepare the slurry, would consume a considerable part of the energy released from the fuel burning. Thus, one-step slurry gasification becomes a low-efficiency option. However, it has been shown that drying the slurry before the gasification step, combined with efficient energy-recovery system, led to relatively high overall power generation efficiency [42]. The present study investigates how the overall power generation efficiency is affected by the amount of water added to the feeding MSW.

Basically, the mentioned gasification process is a partial combustion of the solid carbonaceous fuel aiming to convert it to fuel gases [43, 44]. Among the applications of the

fuel gas, it is heating and power generation. For the specific application in Fischer-Tropsch process, further processing has to be applied in order to achieve synthesis gas (syngas) specifications.

One of the first products of the gasification process was called “town gas” or fuel-gas, used mainly in the USA and Europe at the beginning of 19th century, for lighting and heating. Coal was the usual fuel. Further improvements on gasification were applied, and during World War II gasifiers were fit to vehicles able to consume the produced gas. Fisher-Tropsch process was also used to convert coal in useful liquid hydrocarbons. These developments continued during the second half of 20th century in countries with sizable coal reserves but few oil ones. Finally, by the end of the 20th century, the gasification processes started to be used in power generation with the development of the first power generation plants based on the Integrated Gasification Combined Cycle (IGCC) [45].

There are few alternatives to use the fuel gas from gasification. The first one is to burn it in boilers to produce steam. Alternatively, one might use the gas to drive cycles or processes aimed directly to power attainment. A third possibility employs plasma technology, where high temperature of the plasma arc greatly reduces the polluting or health-hazardous potential of substances or compounds in the fuel and the solid residues are produced in the form of a vitrified slag [46]. However, that last alternative brings unfavorable economic factors and should be used only in very special conditions or cases.

Historically, various gasifier concepts were developed. Breault, R.W. [45] describes some of the most important among those concepts. A brief description of those is presented in Table 2.

Table 2. *Examples of gasifiers developed up to 2010 (Source: Breault, R. W. Gasification Processes Old and New: A Basic Review of the Major Technologies. Energies [Online] 2010, 3, 216-240)*

GASIFIER	DESCRIPTION	APPLICATION
GE Energy	A coal-water slurry fed, oxygen-blown, entrained-flow, refractory-lined slagging gasifier	Up to 2010, there are 64 plants operating and six plants in planning.
ConocoPhillips E-Gas	Originally developed from 1987 through 1995. It is a two-stage gasifier with 80% of feed to first stage (lower). The gasifier is coal-water slurry fed, oxygen-blown, refractory-lined gasifier with continuous slag removal system and dry particulate removal.	There is one plant operating and six plants in planning.
Shell	Has its roots dating back to 1956 leading to their first demonstration facility in 1974. Coal is crushed and dried and then fed into the Shell gasifier as a dry feed. The gasifier is an oxygen-blown, water-wall gasifier eliminating refractory durability issues.	There are 26 Plants operating and 24 plants in planning.
Siemens	Initially developed in 1975 and first demonstrated in 1984. The gasifier is a dry feed, oxygen-blown, top fired reactor with a water wall screen in the gasifier.	Up to 2010, there is one plant operating and one plant in planning.
KBR Transport	It operates air blown for power generation and oxygen for liquid fuels and chemicals. It is a non-slagging gasifier with no burners and utilizing a coarse, dry low rank coal feed.	Presently, there is one IGCC in design.
British Gas Lurgi	Developed during the period from 1958 to 1965. It is a dry feed, oxygen-blown, refractory-lined gasifier.	A demonstration plant operated from 1986 to 1990, and the first commercial plant operated from 2000 to 2005.
Multipurpose Gasifier	An oxygen-blown, down fired, refractory lined gasifier good for wide range of feed stocks including petroleum coke and coal slurries as well as waste.	A reference plant has been in operation since 1968.
Lurgi Mark IV Gasifier	Has a dry feed system with lock hoppers to provide the pressure seal. It is an oxygen blown, dry bottom gasifier.	There are 8 plants operating.
Mitsubishi Heavy Industries Gasifier	Based upon the Combustion Engineering air-blown slagging gasifier. It has a dry feed system. It is an air blown two-stage entrained bed slagging gasifier utilizing membrane water-wall construction.	Up to 2010 there was one demonstration plant in operation.
U-Gas	A fluidized bed gasifier incorporating a dry feed system. It is highly efficient in either the air or oxygen blown configuration producing a non-slagging/bottom ash.	Up to 2010 two plants were in operation.
High Temperature Winkler Gasifier	A fluidized bed gasifier utilizing a dry feed and operating either in the oxygen or air-blown modes. It produces a dry bottom ash.	A demonstration plant shut down in 1997.
PRENFLO™ Gasifier/Boiler	A pressurized entrained flow gasifier with steam generation. It is an oxygen blown, dry feed, membrane wall gasifier.	The technology is used in world's largest solid-feedstock-based IGCC plant in Spain.

Besides gasification, combustion and pyrolysis are other two options for the thermochemical conversion of MSW.

Waste-to-Energy (WtE) plants usually apply steam cycles with almost complete combustion of that residue. Their sizes are in the range between 35MW (LHV base) and 90MW. The typical small thermal input size has several effects on the WtE performances due to many reasons. Among them the decrease in efficiency because steam turbine performance decreases with the size, requires relatively larger air excesses due to unfavorable volume to surface ratio in the combustion chamber, and lower auxiliary device performances, since those also decrease with equipment sizes [46].

Besides that, conservative steam parameters compose another limitation to reach higher efficiency values. For the Rankine cycle, efficiency increases for higher steam temperatures. However, the heat transfer surfaces of WtE boilers must face severe, high temperature, acidic corrosion, caused by both the metal chlorides in the fly ash and the high concentration of hydrogen chloride (HCl) in the flue gas. The corrosion rate increases with temperature, hence, to limit corrosion, the temperature of the surfaces must be limited. This consideration applies both to evaporating and superheating surfaces, thus, setting limits to superheating temperature [46].

Furthermore, Rankine cycle efficiency is also improved by lowering the pressure at the condenser. In traditional WtE plants, air cooled condensers, working under relatively high pressure, are often applied. For large installations, larger surfaces of air cooled condensers or the use of water cooled condensers may lower the condensing pressure and hence improving the efficiency.

Additionally, for facilities with low processing capacity (100,000 to 150,000 Mg/y), the in-plant consumption represents a quite important fraction of the gross power. Depending on the plant size the overall fraction of the electrical power for in-plant consumption is 10 to 15%, which may increase up to 21% when waste pre-treatment consumption is required to feed fluidized bed. An alternative to improve the performance is the integration of municipal waste incinerator with combined steam gas cycles [46].

For both combustion and gasification (with fuel gas consumed in a boiler), it is possible to summarize that large scale plants might reach between 30 and 31% net electric efficiency, while small/medium size ones, net electric efficiency might achieve from 20 to 24%. Studies related to gasification with fuel gas in devices aimed directly to power attainment, such as gas

turbines and internal combustion engines, provided efficiencies similar to those of conventional plants based on incineration [46].

Another line of research for power generation involves pyrolysis. It is a thermal process taking place with complete or almost complete absence of oxygen, and using an external source to provide the required energy. It produces three output streams: gas, liquid (oil) and solid (char). Due to the absence of oxygen, no oxidation occurs, while the feeding organic material undergoes a thermal degradation. Pyrolysis application for energy recovery from wastes is limited to few specific situations. While a large development of biomass pyrolysis was carried out in the last years, pyrolysis of waste is mainly at research and development stages [46].

4 MATHEMATICAL MODEL

The study used mathematical simulators of both the dryer and gasifier (CeSFaMB©) and the gas turbine combined process (IPES©), which are briefly described in subsequent sections. Additional information on CeSFaMB© can be found in Appendix 1.

4.1 DRYER AND GASIFIER SIMULATION - CESFAMB©

The CeSFaMB© (Comprehensive Simulator of Fluidized and Moving Bed equipment) is a computational model based on a mathematical model developed for the representation of bubbling and circulating fluidized bed equipment, as well as updraft and downdraft moving bed and entrained flow equipment. Among these industrial and pilot units, there are furnaces, boilers, gasifiers, dryers, and reactors.

CeSFaMB© model is one-dimensional, but including all relevant phenomena. The justification for this approach can be found in the literature [49].

The assumption of the first-order model may seem simple, but it must be realized that the processes occurring inside bubbling fluidized bed combustion chambers, boilers, or gasifiers can involve up to five physical states, dynamics of those phases and iterations among them, heat and mass transfers between phases, heat transfer between phases and walls (including tubes in case of boilers), generation of finer particles due to attrition among them as well due to heterogeneous chemical reactions, as well several other processes. Additionally, the model considers about one hundred possible homogeneous and heterogeneous chemical reactions, including processes such as pyrolysis, drying of solid fuels, and sulfur absorptions in cases of limestone or dolomite are added to the reactor. The structure considers 18 gaseous and 14 solid chemical components. Most chemical components are present in all physical states.

The mass and energy balances at each point of the equipment lead to a system of nonlinear and highly coupled differential equations.

Among the most important information provided by the simulation are:

- Profiles of concentration and mass flow rate of 18 gas components (Ar, CO_2, CO, O_2, N_2 and H_2O, H_2, CH_4, SO_2, NO, N_2O, NO_2, HCN, C_2H_6, H_2S, NH_3, C_2H_4, C_3H_6, C_3H_3, C_6H_6, tar) along the bed in the bubble phase and emulsion;
- Profiles of concentration and mass flow of these species along the freeboard region.
- Composition, circulation rates and particle size distribution of all solid species in the bed. The possible solids are carboniferous, limestone or dolomite (or a mixture of both), and inert;
- Profiles concentration, mass flow and particle size distribution of all the solid species along the freeboard region;
- Gas temperature profiles in the emulsion, bubble gas, carboniferous, limestone or dolomite (or a mixture of both), and solids inert along the bed;
- Gas temperature profiles and solid phases of three possible across the freeboard region;
- All parameters related to fluidization dynamics at each bed point, such as bubble sizes and velocities, mass flow through each phase, particle circulation rates, etc. For circulating beds, the fluidization parameters are also calculated and reported;
- Pressure drops on the manifold and bed;
- Typical engineering parameters such as efficiency, heat losses to the environment, external wall temperature profiles, adiabatic flame temperature of the gas produced (if any), the compositions of the outlet streams on several different bases, drag and elutriation parameters, among other details.

In the case of boilers, the simulation gives detailed profiles of temperature of the wall of the tubes in the bed and freeboard region. In cases of circulating beds or if particles collected in the cyclone system are totally or partially recycled to the bed, the simulation provides various data regarding the operation of the cyclone system, as well as the composition and particle size distribution of the bed solids. If tubes (one or several sets) are immersed in the bed, the program shows the erosion rate of the tube walls. If intermediate injections are used and withdrawals of gas and the bed and/or freeboard region, the effects of these intermediates fluxes in the process are computed;

As input data, the program requires:

- Parameters required to set the numerical convergence and solution of differential equations;

- Description of the equipment (equipment type, hydraulic diameter and bed height, among other geometry parameters);
- Distributor description (distributor type, orifice diameter, etc.);
- Parameters related to the use of cyclones for recycling of particles;
- In case of boilers, parameters related to tube banks (diameters, pressure of the fluid inside the tubes, number of tubes in each bank, etc.);
- Parameters related to the use of a "cooling jacket" (fluid used, fluid inlet temperature in the cooling jacket);
- Characterization of the gases injected in the distributor, as well as in intermediate injections (composition, mass flow, temperature, etc.);
- Parameters of operation of the equipment (such as internal pressure);
- Characterization of the solid components injected into the equipment, whether carbonaceous materials, limestone / dolomite or inert materials (particle size distribution, temperature, mass flow, composition, amount of added water to form slurries, etc.).

These and other input data will be properly characterized in subsequent sections.

4.2 THERMODYNAMIC PROCESS SIMULATION - IPES©

The IPES© (Industrial Plant and Equipment Simulator) is a computational code based on a mathematical model developed for simulating thermodynamic processes and equipment. The program includes the basic equations related to the mass and energy balances around each process equipment, as well as lists all the input and output streams of all the equipment, in order to simulate the whole process. Applying the 1st and 2nd laws of thermodynamics, the result is a system of equations with number of unknowns equal to the number of equations to be solved.

The program can simulate various equipment, among them: turbines, compressors, pumps, nozzles, mixers, splitters, heat exchangers and valves. The data required by the program for the simulation include description of each of the equipment (equipment type,

input and output currents, efficiency, etc.) and, when imposed or known, the description of each stream (mass flow, temperature, pressure, and composition).

The main data obtained after the simulation include the temperature, pressure, composition, saturation pressure, enthalpy, entropy, exergy, specific heat and its integral, combustion enthalpy, as well flame temperature of each stream. Additional information are efficiency of heat exchangers and process 1st and 2nd law efficiencies.

The most relevant data for this study will be properly characterized in subsequent sections.

5 STUDY PARAMETERS

The basic main assumptions applied to the present investigation are:

a) The gasifier and dryer operate as a bubbling fluidized bed equipment, but other techniques, such as circulating bed or even entrainment flow, could be applied as well. It is believed that such choices would not drastically modify the main conclusions of the present work. On the other hand, it should be stressed that bubbling bed reactors are less stringent than those other techniques regarding the range of feeding particle size and density. Other main advantages of bubbling fluidization over other techniques are [47-50]:
   - The bed and freeboard normally operates at relatively low and uniform temperatures. This brings savings in materials and insulations.
   - Relatively high response time when variations of temperature or other parameters occur, which allows the application of less expensive controlling instrumentation.
   - High residence time inside the bed, which leads to higher fuel conversion.
   - Possibility of adding sulfur absorbents, such as limestone or dolomite, into the bed, which allows for savings in effluent gas cleaning.
   - If denser particles than the average, enter a bubbling fluidized beds, they would drop to the bottom of the bed and would be removed by proper mechanical means without interrupting the equipment operations. This is expected when working with diverse materials such as those composing MSW.

b) MSW includes a very wide range of possible materials. The average characteristics of such residues also vary with the region and economic conditions of the consuming population. The work of Gidarakos et al. [17] was used due to its coherence and completeness of data. Those are reproduced in Table 3.
c) The basic shape of MSW has been set as cylindrical, typical of fibrous materials, because a substantial portion of MSW is composed by cardboards, paper, and food residues. However, other choices for the basic fuel shape should not significantly affect the results presented here.
d) Likewise biomass, the apparent and real densities of wet MSW have been assumed as 720 and 1394 kg/m^3, respectively.

e) The rate of wet MSW consumption was set at 28.45 kg/s. Such MSW rate might be generated by 3 million inhabitant cities, approximately [11]. The dryer operating pressure is slightly above 2 MPa. Scaling up or down regarding the MSW feeding rate should not compromise the main conclusions arrived here. Nevertheless, the present results can be easily scaled up or down and such should not invalidate the main conclusions of the present work.
f) The maximum dry-solid content in a slurry able to be handled by commercial pumps have been observed. That value should be around 50% [51].
g) As commented, the gas leaving the gasifier should be cleaned to decrease particle content and their sizes to values acceptable for injections into commercial gas turbines. In addition, the alkaline concentrations in that gas must also be decreased for the same aim [30-32]. Ceramic filters might be applied to tar removal and temperature drop to 800 K - which is below the dew-points of alkaline components - allowing significant decrease in the concentrations of those species in the gas stream [33].
h) The isentropic efficiency of compressors is assumed as 87% for compressors [52].
i) The isentropic efficiencies of both, gas and steam turbines are assumed as similar to compressors, 87%.
j) The maximum temperature of streams leaving axial compressors is taken as 950 K [53].
k) Pumps isentropic efficiency assumed as 95% [54].
l) Minimum temperature difference between heat-exchanging streams set as 10 K.
m) Maximum injection temperature into turbines set at 1700 K.
n) High-temperature heat exchangers can be used in some particular situations. Nonetheless, some precaution as to minimize the regions where those must be applied is always advisable to avoid excessive capital and maintenance costs. [55].
o) The average pressure loss in heat exchangers are assumed as 10 kPa.

Modifications on those assumptions might be made in future investigations. Despite that, the main results achieved here should not be drastically altered.

No economic considerations or computations are part of the present work.

The evaluation of the process studied here requires more detailed descriptions related to the consumed fuel and involved equipment. Among the most important information are the

dryer and gasifier geometric characteristics, their basic operational parameters, as well as the characterization of the consumed fuel. These are presented in the following sections.

Table 3. *Main characteristics of the fuel (MSW) consumed by the process*

Physical Characteristics of the Fuel:	
Bulk Density	200 kg/m^3
Apparent Density	720 kg/m^3
True Density	1394 kg/m^3
Sphericity	0.70
Shape	Cylindrical
Particle average diameter	2 x 10 $^{-3}$ m
High heating value (dry basis)	22.30 MJ/kg
Proximate Analyses (wet basis)	
Moisture	36.72 %
Volatile	52.64 %
Fixed Carbon	6.02 %
Ashes	4.62 %
Ultimate Analyses (dry basis)	
Carbon (C)	53.00 %
Hydrogen (H)	7.32 %
Nitrogen (N)	1.32 %
Oxygen (O)	30.96 %
Sulfur (S)	0.10 %
Ash	7.30 %

5.1 DRYER DESCRIPTION

As seen before, the dryer is assumed to be a bubbling fluidized bed. Its distributor design includes flutes with holes through which the fluidization gas (stream 28, Fig. 3) is injected.

The dryer has a non-circular cross-sectional geometry, with bed height of 3 m and hydraulic diameter of 4 m. The freeboard region is 7 m high, with a hydraulic diameter of 8 m. The distributor consists of 50,000 flutes with 10 orifices per flute. Each orifice has 3 mm of diameter. The internal and external diameters of the flutes are 12.7 and 13.2 mm, respectively.

Water and wet MSW are mixed to form the slurry, which is pumped 0.5 m above the distributor. Many of the above geometric and operational characteristics have been found after an optimization, as described ahead.

5.2 GASIFIER DESCRIPTION

The gasifier has a non-circular cross-sectional geometry. Bed height and hydraulic diameter are both 4 m, and freeboard height and hydraulic diameter are respectively 10 and 4 m. The distributor in this case has the same characteristics of the one used in the dryer.

The rate of 18 kg/s of dry MSW is fed into the gasifier at 2 m above the distributor. Air is injected through the distributor at 765 K. The operating pressure of the gasifier is 2 MPa. To be on the conservative side, the temperature of feeding dry MSW is assumed as 290 K. However, that fuel leaves the dryer at higher values, as described below.

Again, many of the above geometric and operational characteristics have been found after an optimization, as described ahead.

Figure 5 shows a draft of the main components of the reactors of both dryer and gasifier.

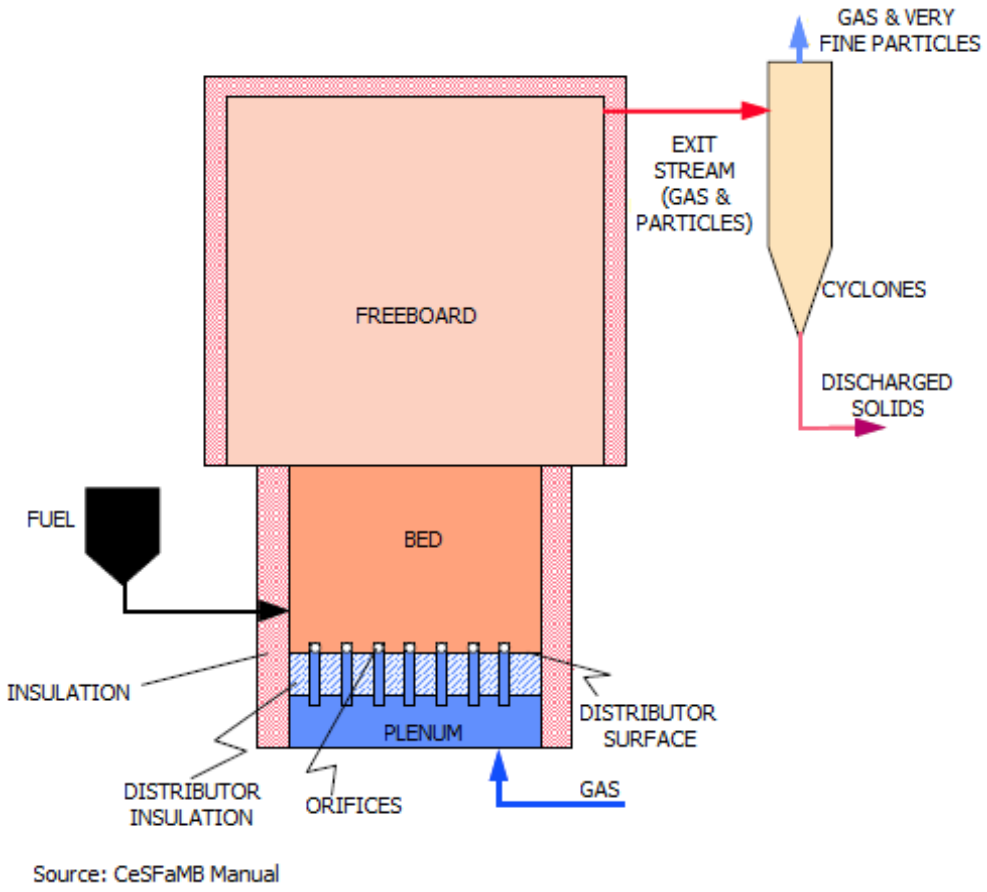

Figure 5. *Dryer and Gasifier's draft*

5.3 Power generation Process

The process configuration is shown in Figure 3. In the process modeling, pump 17 is responsible to pressurize the MSW slurry before injection into the dryer. Since water is the fluid added to the wet MSW, it is assumed that it is pumping water. Since the slurry behaves as incompressible fluid, that should not impact on the conclusions arrived here.

5.4 Remarks about Efficiency

During the development of the work and presentation of the results, different concepts of efficiency were employed, as summarized below:

a) Gasifier hot efficiency: Ratio between the rates of combustion and sensible enthalpies of gas stream leaving the gasifier computed at the temperature, pressure, and composition as found at the exiting point from the equipment and the total rate of energy inputted to the equipment;
b) Gasifier cold efficiency: Ratio between the rate of combustion enthalpy of the dry and tar-free gas stream leaving the gasifier computed at 298 K and 101.325 kPa, and the total rate of energy inputted to the equipment;
c) Process 1st Law efficiency: Ratio between the net useful mechanical power output and the rate of energy inputted by fuel;
d) Process 2nd Law efficiency: Ratio between the net useful mechanical power output, and the rate of exergy inputted by fuel;
e) Gasifier exergy efficiency: ratio between the rate of exergy of the produced gas leaving the gasifier and the sum of exergy rates of all streams entering the gasifier.

6 METHODOLOGY

The present work evaluates the relationship between the amount of water added to the MSW to form the slurry and the exergy efficiency of the power generation process, which is the best indicator for the amount of energy available to perform work. Further details about the concepts of exergy and exergy efficiency, as well as their due equation, can be found in the literature [44]. For the study, the conditions pre-established in de Souza Santos and Ceribeli [42] were used as baseline, and the four steps were followed: gasification optimization; process first optimization; dryer optimization and; process second optimization.

6.1 GASIFIER OPTIMIZATION

The exergy efficiency has been chosen as objective function during the gasifier optimization. The gasifier bed diameter and the mass flow of the air injected in it have been selected as variables. Other variables - such as bed height and various characteristics of the equipment, gasification pressures, fuel particle size distribution - could be included as variables as well. However, the selected ones are among the most influential in the gasification process. Additionally, each new variable included would multiply the number of simulations and bring complications on understanding the effect of each one in the whole process. Future works might consider adding variables for the gasifier optimization.

Since dried fuel enters the gasifier, it can be optimized independently from the dryer and process optimizations.

The gasifier cold efficiency could also be taken as objective function. However, the exergy efficiency includes the temperature of exiting gas, and that constitutes an important fraction of the energy carried by the produced gas stream, which is used to drive the Rankine cycle (Figure 3, equipment 11 to 15).

Graphs of the gasifier exergy efficiency, cold efficiency and average temperature inside the bed were plotted. Also, some of the simulator outputs data and graphics are presented.

6.2 PROCESS FIRST OPTIMIZATION

With the complete characterization of the gasifier exhaust gas, and using the IPES© simulator, it was possible to obtain the characteristics of all the streams involved in the process. Having in mind the process shown in Figure 3, the second step was the optimization of the whole power generation process. That optimization aimed to the following:

a) Reduction of mass flow rate of the air stream feeding the combustor (Streams 1 and 2). Since it is compressed at relatively high pressure, this could lead to energy savings;

b) Reduction of mass flow rate, and whenever possible the temperatures of water heading to cooling towers from the energy recovery processes (Streams from 7 to 9 and 21 to 23). This measure will prevent too much power used by pumps as well energy losses to environment.

c) Reduction of pressure from streams leaving the steam turbines (Streams 11 and 18, and consequently 12 and 19). In this way, it will be possible to increase the steam turbine power outputs.

d) Increasing the pressure of streams injected into the steam turbines (Streams 10 and 17, and consequently 13 and 20). The expected effect is similar as reducing the pressure on the exit of the turbines.

6.3 DRYER OPTIMIZATION

Once the maximum process efficiency (excluding the drying process) was reached, the characteristics of Stream 28 were known. That allowed the dryer optimization for each case of water content in the feeding slurry.

Similarly to the procedure used during the gasifier optimization, a network was built having the percentage of water in the slurry and dryer diameter as variables. At each instance, successive iterations aimed to operate the dryer with the minimum mass flow of gas in order to achieve complete drying of the fuel (also using the simulator CeSFaMB©). That would minimize the power required by compressor (equipment 10, Figure 3).

The dryer diameter must be within a range that allows operations within feasible fluidization conditions. Few of the most relevant simulator outputs data and graphics are presented.

6.4 Process Second Optimization

After each step of dryer optimization, the process was simulated again, with the adjustments for the mass flow rate of gas feeding the dryer (using the simulator IPES©). The characteristics of all the streams involved in the process are finally presented.

Moreover, the process was simulated for different dry solid content in the slurry (but for a unique dryer internal diameter). For each condition, the value of the exergy efficiency was obtained. With the results, a graph was created for a better visualization of the influence of the amount of water added to the MSW in the exergy efficiency of the process.

A simplified diagram of the optimization flowchart is shown in Figure 6.

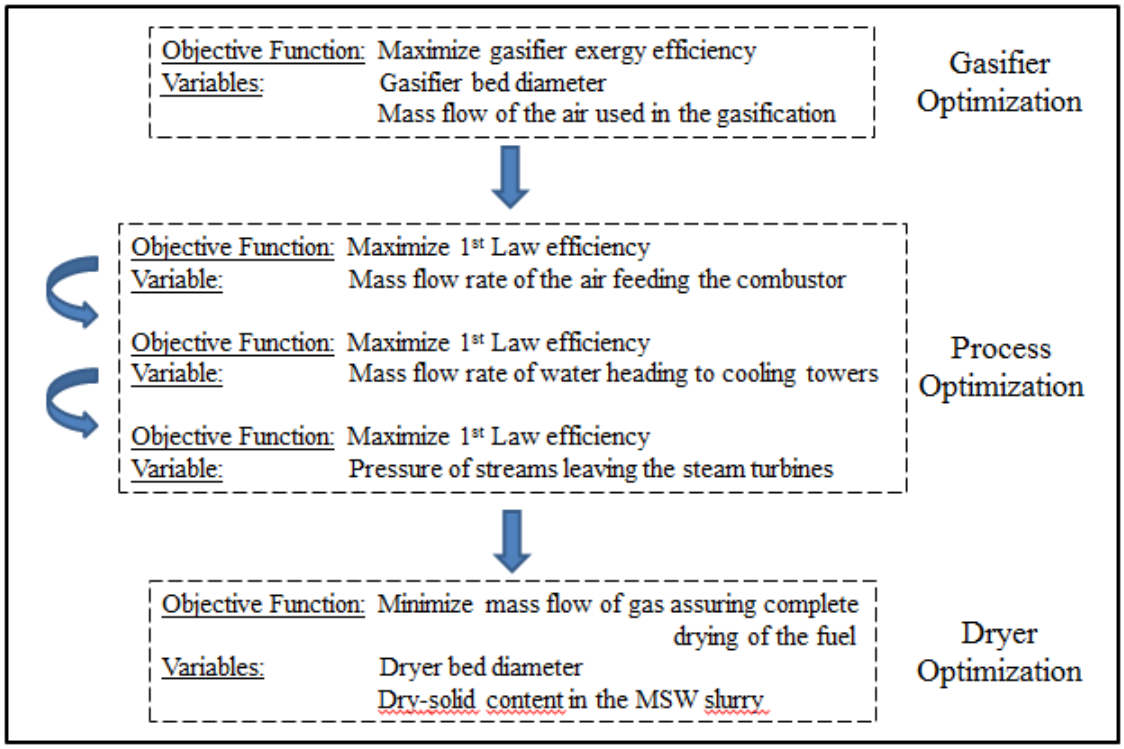

Figure 6. *Optimization flowchart*

7 RESULTS AND DISCUSSION

The gasifier optimization progressed by studying the influences of both bed diameter and air injection rate in the gasifier efficiency. The results obtained for exergy efficiency, cold efficiency and average temperature inside the bed are summarized respectively in Figures 7 to 9. Lacks of data at few points on those graphs are due to operations that:

a) Led to slugging-flows, or when the superficial velocities inside the bed are outside the bubbling fluidized conditions;
b) Allowed temperatures surpassing ash-softening limits;
c) Led to unsteady-state operations. For instance, when too much solid is elutriated or leaving the equipment, thus not allowing the bed level to be kept constant.
d) Provided too low efficiencies.

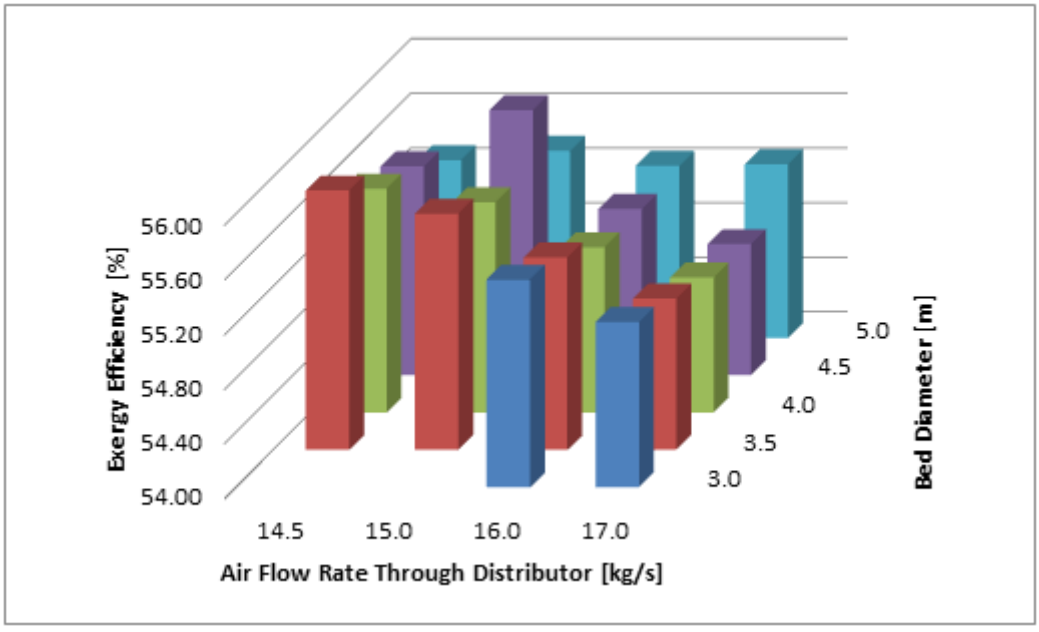

Figure 7. *Exergy efficiency against bed diameter and rate of air injected into the gasifier*

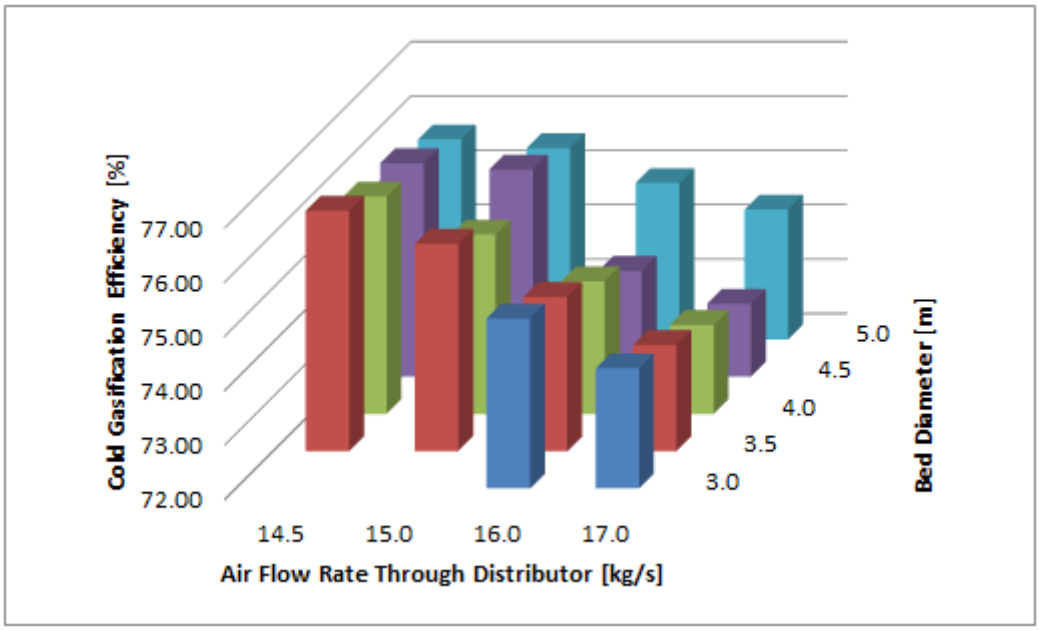

Figure 8. *Cold gas efficiency against bed diameter and rate of air injected into the gasifier*

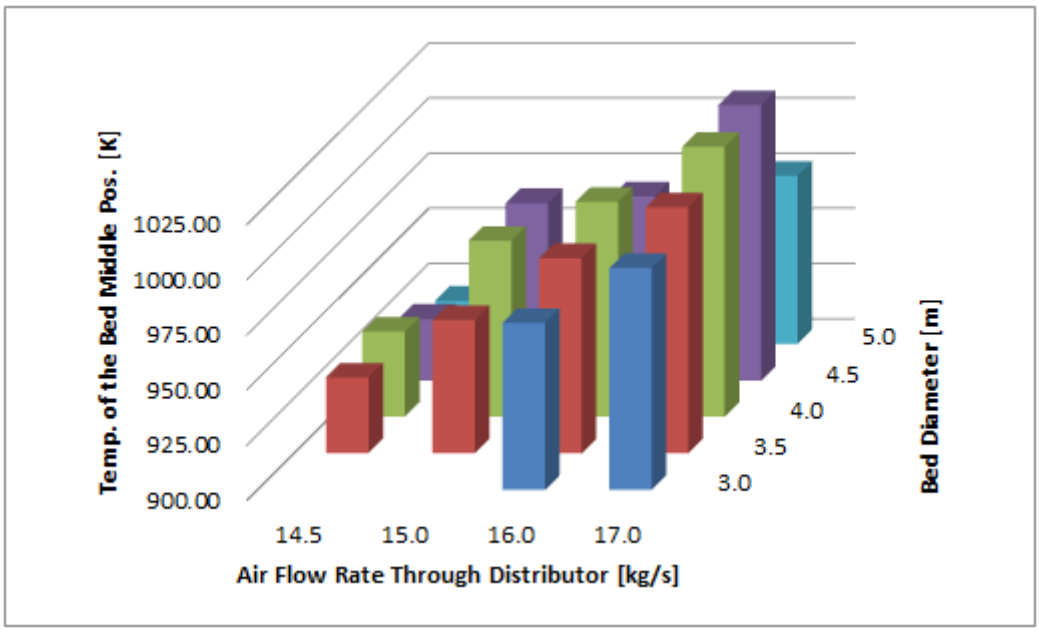

Figure 9. *Average temperature inside bed against bed diameter and rate of air injected into the gasifier*

The highest gasifier exergy efficiency was achieved for bed diameter of 4.5 m and air flow of 15.0 kg/s. The main gasifier output parameters are listed at Table 4.

Table 4. *Main output parameters from gasifier*

Main Output Parameters	Values
mass flow of gas leaving the equipment (kg/s)	31.83
mass flow of solids discharged from the bed (kg/s)	0.89
mass flow of solids reaching the top of freeboard (kg/s)	0.85
fluidization superficial velocity (bed middle) (m/s)	0.14
average temperature at the middle of the bed (K)	980.33
average carbonaceous particle diameter in the bed (mm)	1.25
average carbonaceous particle diameter at freeboard top (mm)	0.13
carbon conversion (%)	79.24
pressure loss at the distributor (kPa)	0.01
pressure loss in the bed (kPa)	24.31
rate of energy input by fuel to the equipment (MW)	376.93
total rate of energy input to the equipment (MW)	384.28
combustion enthalpy of hot gas (MJ/kg)	10.23
combustion enthalpy of cold gas (MJ/kg)	9.50
rate of energy output by hot gas[a] (MW)	325.71
rate of energy output by cold gas[b] (MW)	291.34
hot efficiency (%)	84.76
cold efficiency (%)	75.81
exergy flow brought with the dry fuel (MW)	566.70
exergy flow brought with the injected gas (MW)	7.37
total entering exergy flow[c] (MW)	574.10
exergy flow leaving with the gas (MW)	321.16
total exiting exergy[d] (MW)	322.90
ratio between total leaving and entering exergy flows (%)	56.24
ratio between the exergy leaving with the gas and the total entering exergy (%)	55.94

[a]"Hot gas" refers to the temperature, pressure, and composition as found at the exiting point from the gasifier. [b]"Cold gas" refers to the gas properties if at 298 K, 101.325 kPa, dry and tar free. [c]Sum of exergies brought by gases, liquids, or solids injected or fed into the gasifier. [d]Sum of exergies carried by gases, liquids, or solids leaving the gasifier.

Figures 10 and 11 show the temperature profiles of various phases in the gasifier bed and freeboard, respectively. The variations of temperatures around the position of 2 m are due to the fuel feeding.

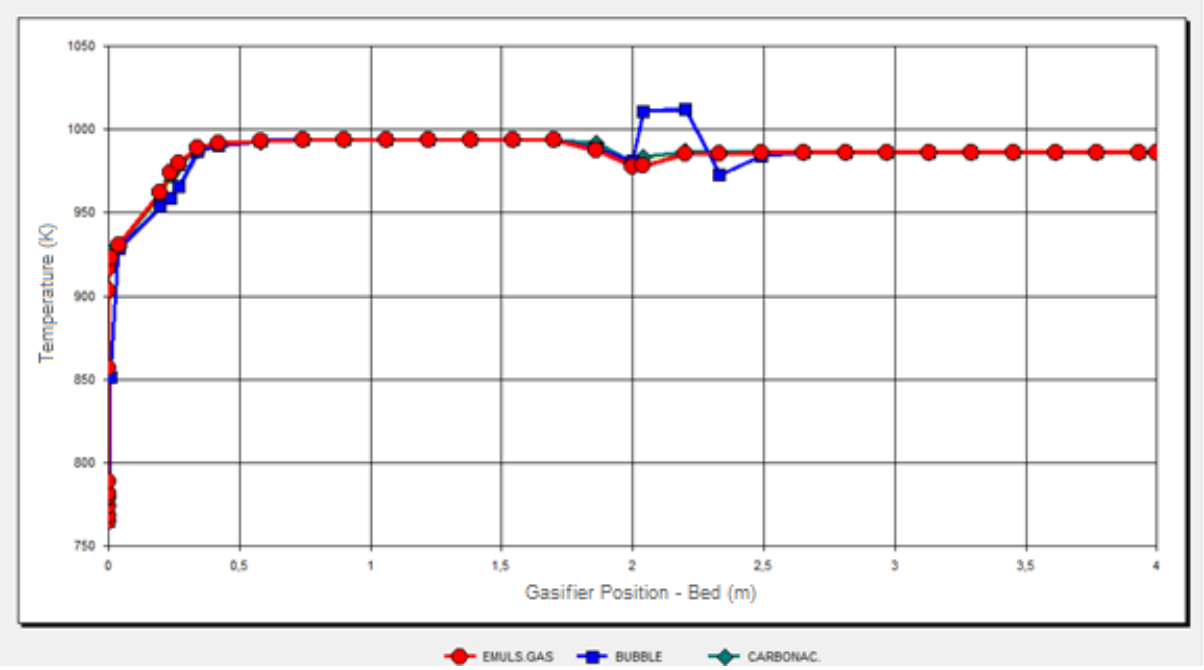

Figure 10. *Temperature profiles at the gasifier bed region*

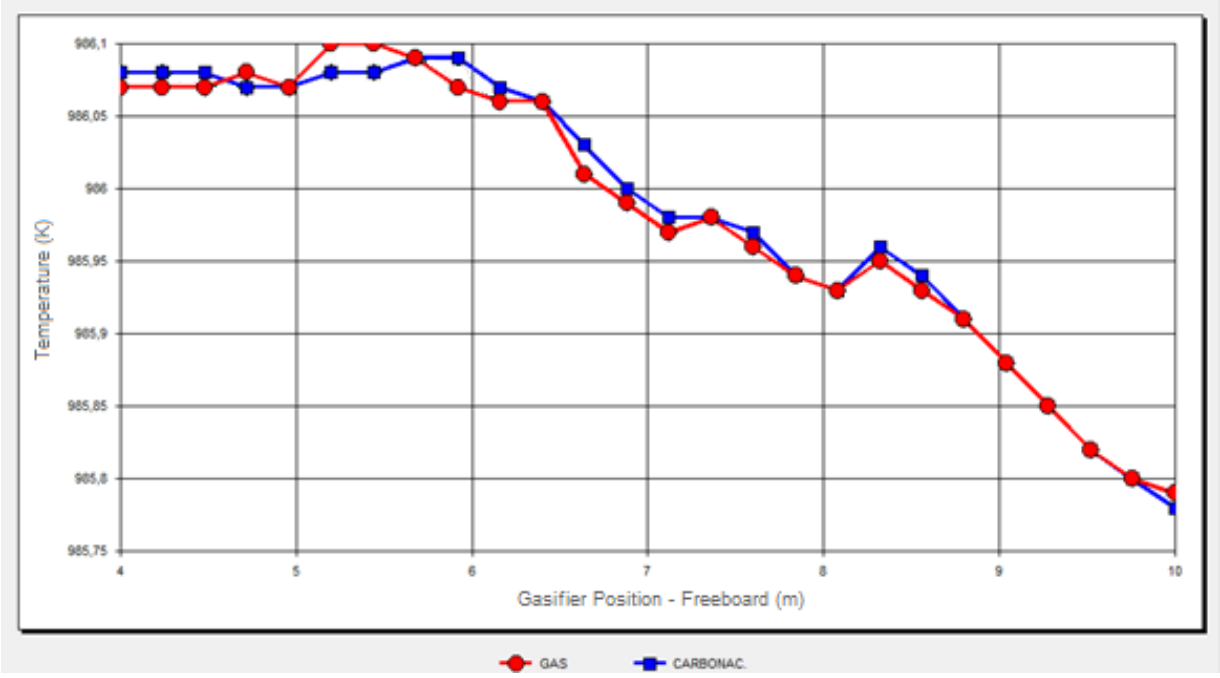

Figure 11. *Temperature profiles at the gasifier freeboard region*

Figure 12 shows that no large bubbles are produced, therefore, with no risk of a slugging-flow operation, and Figure 13 illustrates the average concentrations of CO, CO_2, and O_2 throughout the gasifier. The sudden gradient changes are due to the fuel feeding. Oscillatory behavior of bubbles average velocity before reaching the fuel feeding position is mainly due to effects of the software numerical calculation method. Those can be avoided by decreasing the numerical convergence tolerance. However, that would lead to much longer computational times without significant impacts on the main results reported here.

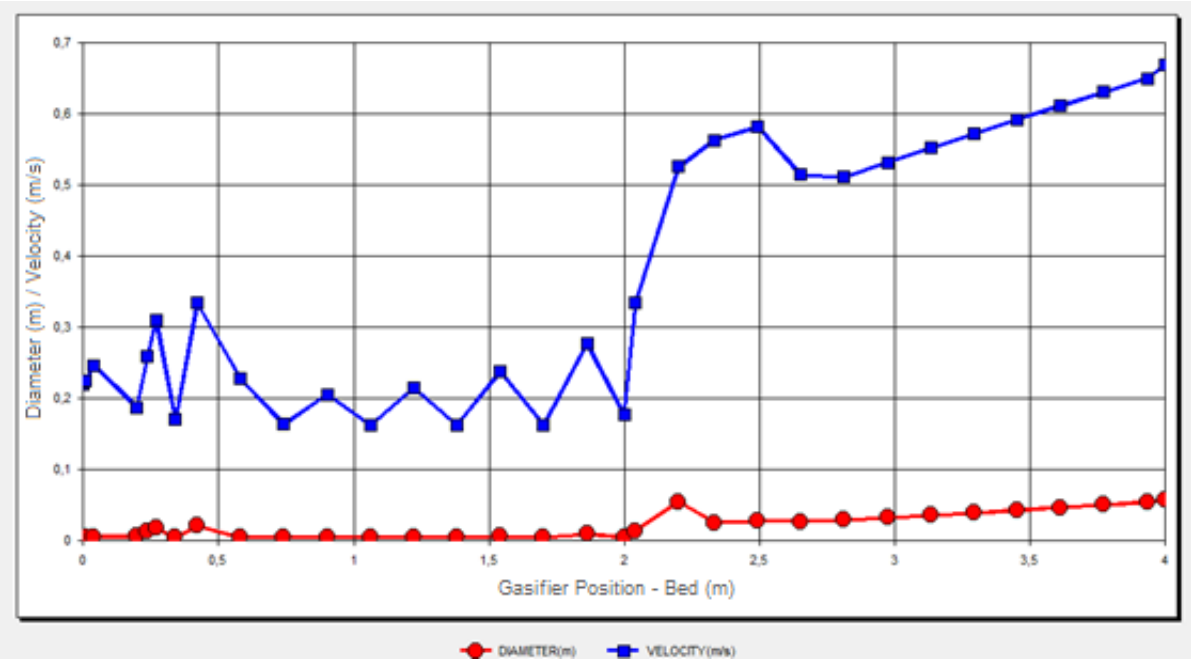

Figure 12. *Bubble sizes and raising velocities through the gasifier bed*

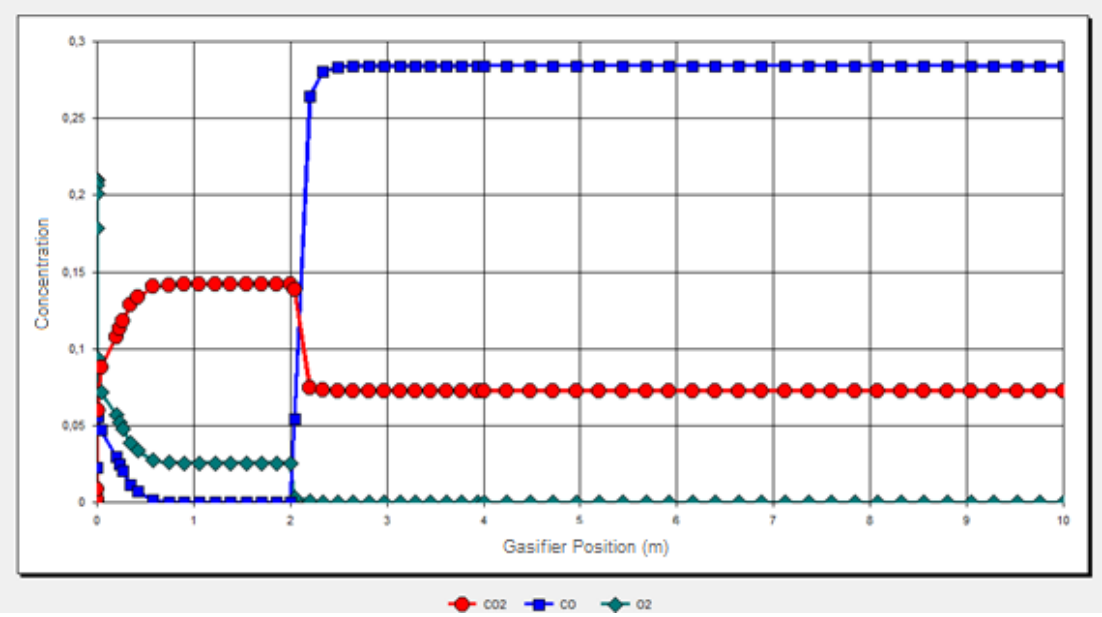

Figure 13. *Concentration profiles of CO, CO_2, and O_2 throughout the gasifier*

Figure 14 shows the evolution of other important fuel gases. The surges of fuel gas productions, around 2 m above the distributor, are due to the pyrolysis of feeding fuel.

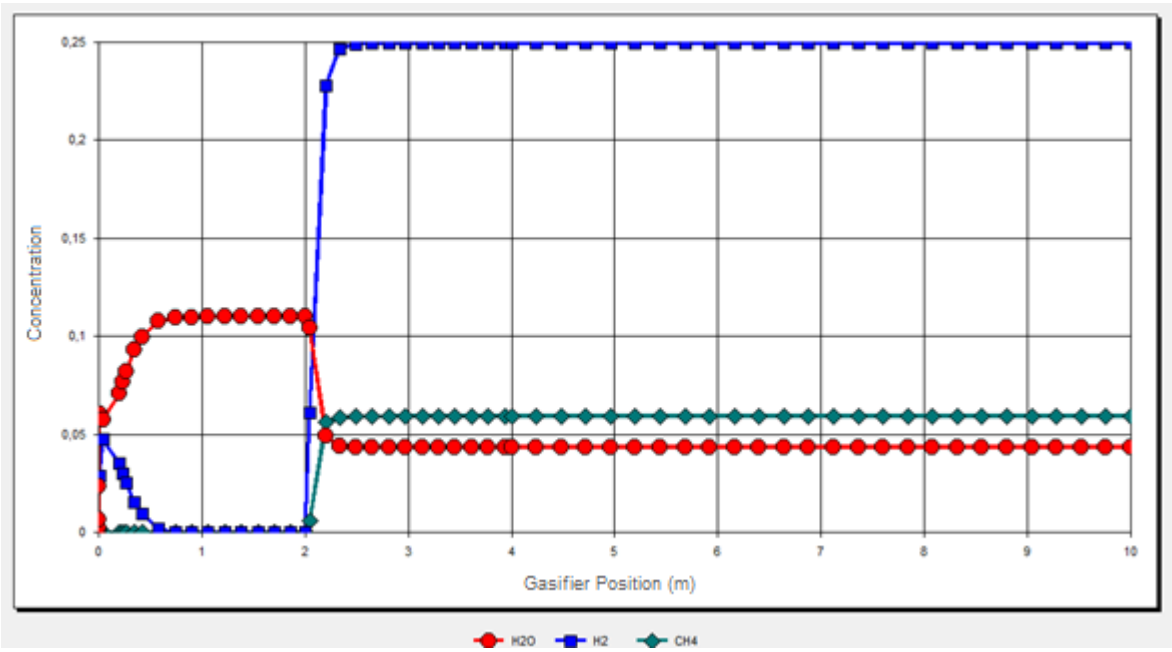

Figure 14. *Concentration profiles of H_2O, H_2, and CH_4 throughout the gasifier*

Figure 15 illustrates the release of tar near the MSW feeding position and its destruction due to cracking and coking inside the bed. This represents an important characteristic of fluidized beds, which avoids the presence of tar in produced gas. Table 5 presents the composition of stream obtained by MSW gasification.

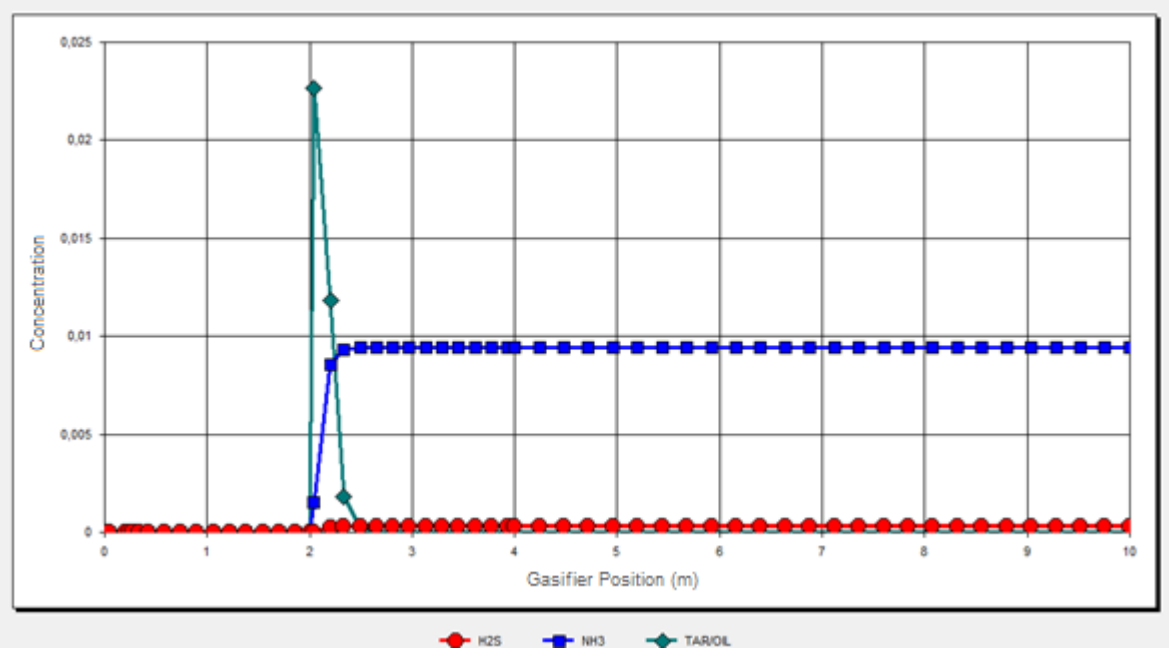

Figure 15. *Concentration profiles of H_2S, NH_3, and tar throughout the gasifier*

Table 5. *Composition of the Gas Exiting the Gasifier*

Chemical Species	Molar Percentage	Chemical Species	Molar Percentage
H_2	24.9388	**CO**	28.3911
H_2O	4.3464	**CO_2**	7.2507
H_2S	0.0306	**HCN**	0.0376
NH_3	0.9427	**CH_4**	5.9295
NO	0.0000	**C_2H_4**	0.1538
NO_2	0.0000	**C_2H_6**	0.1193
N_2	27.7880	**C_3H_6**	0.0057
N_2O	0.0000	**C_3H_8**	0.0054
O_2	0.0000	**C_6H_6**	0.0551
SO_2	0.0053		

In the case of dryer optimization, the bed diameter and solid content in the MSW slurry were taken as variables while the objective was minimizing the fraction of the gas turbine exhaust (Stream 28 on Figure 3) diverted to drying the MSW slurry.

Figure 16 shows the minimum gas flow required for the fuel complete drying as function of those two variables.

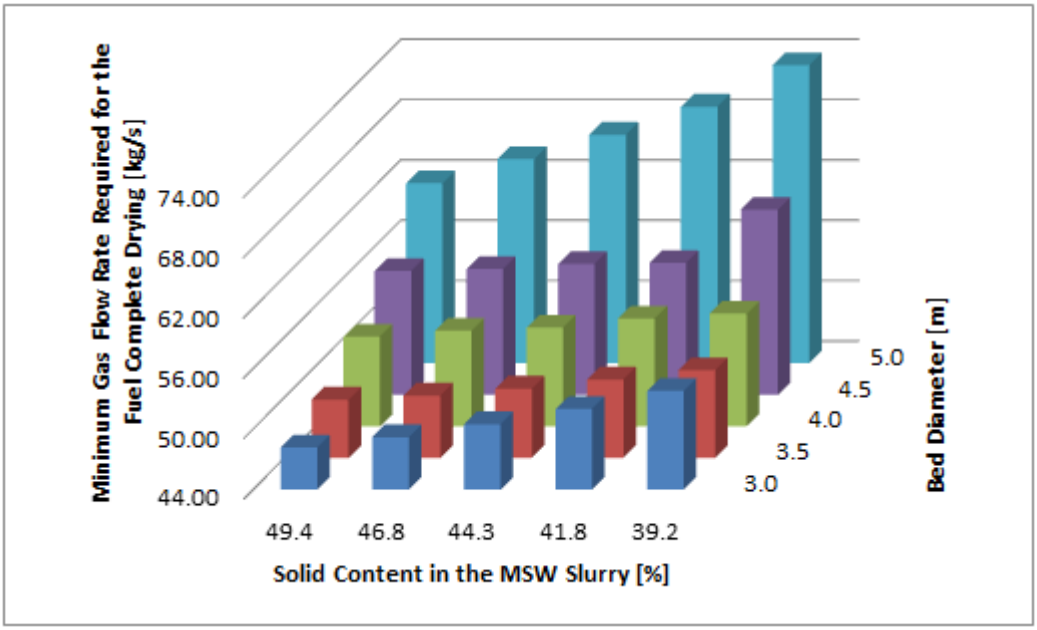

Figure 16. *Minimum gas flow rate required for the fuel complete drying against bed diameter and Solid Content in the MSW Slurry*

The best results for the dryer operation were obtained for a bed internal diameter of 3 m and a solid content in the MSW slurry of 49.4% (an additional amount of 22% water - in mass fraction). Those results are listed in Table 6.

Table 6. *Main output parameters from dryer*

Main Output Parameters	Values
mass flow of gas leaving the equipment (kg/s)	66.67
Concentration of water in the leaving solid (%)	0.00
fluidization superficial velocity (bed middle) (m/s)	0.68
mixing index in the bed	1.00
tar flow at the top of the freeboard (kg/s)	0.00
pressure loss at the distributor (kPa)	1.53
pressure loss in the bed (kPa)	2.46
exergy flow brought with the slurry (MW)	689.70
exergy flow brought with the injected gas (MW)	33.52
total entering exergy flow[a] (MW)	723.20
exergy flow leaving with the gas (MW)	36.20
exergy flow leaving with the dry MSW (MW)	423.70
total exiting exergy[b] (MW)	459.90
ratio between leaving and entering exergy flows (%)	63.59
ratio between the exergy leaving with the gas and the total entering exergy (%)	5.00

[a]Sum of exergies brought by gases, liquids, or solids injected or fed into the gasifier. [b]Sum of exergies carried by gases, liquids, or solids leaving the gasifier.

The temperature profiles of various phases throughout the dryer bed and freeboard are shown in Figures 17 and 18, respectively. As seen, the temperature of gas leaving the dryer is relatively low, thus minimizing the energy losses from the process. This is also shown by the relatively low loss of exergy (5%) carried by the gas leaving the dryer.

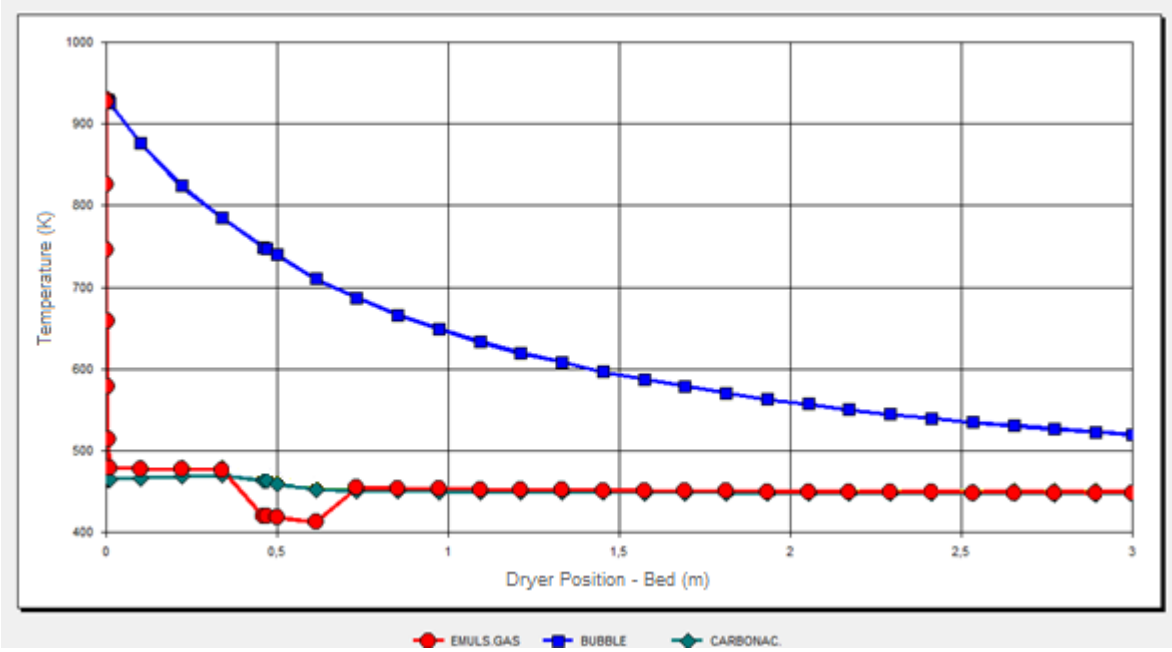

Figure 17. *Temperature profiles at the dryer bed region*

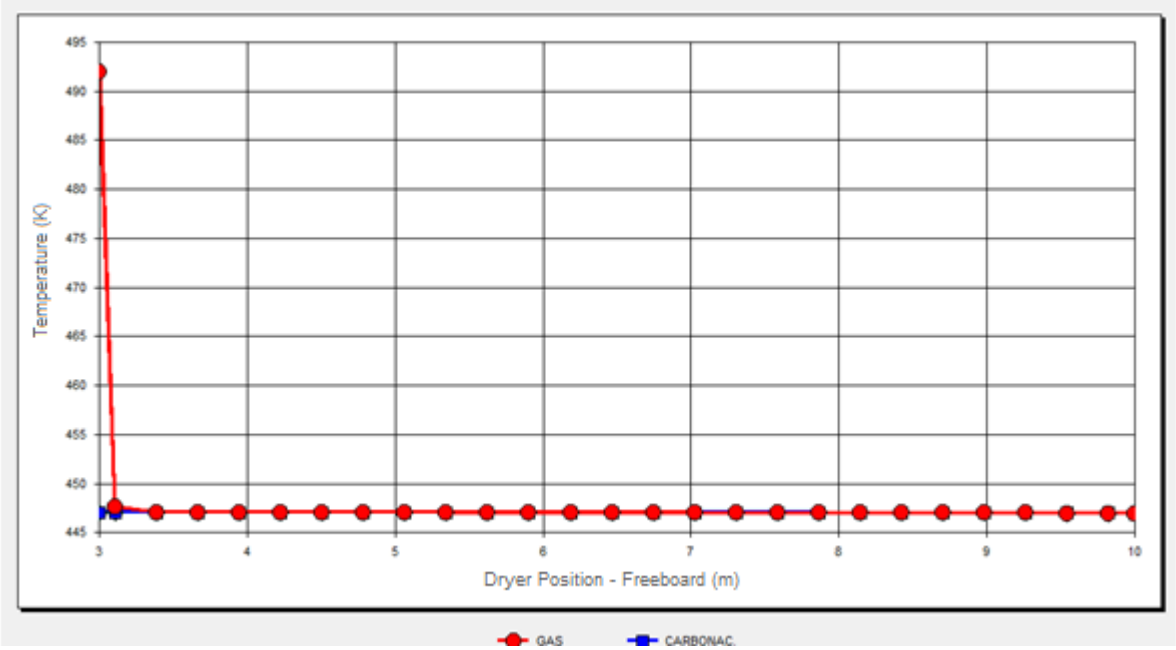

Figure 18. *Temperature profiles at the dryer freeboard region*

After achieving each new optimal dryer operational condition, one additional simulation of the whole power general process was conducted using IPES©.

Table 7 lists the mass flows and properties of each stream of the process. Table 8 appraises information regarding the power input (for pumps and compressors) and output (for

steam and gas turbines) of each equipment of the process. Table 9 summarizes the main overall results achieved.

Table 7. *Description of Conditions at Each Stream of the Proposed Process*

Stream	Working Fluid	Mass Flow (kg/s)	Temperature (K)	Pressure (kPa)
1	Air	210.80	298.00	101.33
2	Air	210.80	762.30	1990.00
3	Gas	31.83	806.00	1990.00
4	Gas	242.63	1699.90	1990.00
5	Gas	242.63	1045.87	120.00
6	Gas	242.63	383.85	110.00
7	Water	364.00	298.00	110.00
8	Water	364.00	298.00	120.00
9	Water	364.00	374.18	110.00
10	Steam	50.00	1028.00	12000.00
11	Steam	50.00	410.37	120.00
12	Water	50.00	370.00	110.00
13	Water	50.00	370.06	12010.00
14	Gas	194.43	383.81	108.00
15	Gas	48.20	383.81	108.00
16	Gas	31.83	985.79	2000.00
17	Steam	2.90	974.00	12000.00
18	Steam	2.90	517.02	490.00
19	Water	2.90	419.76	480.00
20	Water	2.90	419.82	12010.00
21	Water	21.00	298.00	110.00
22	Water	21.00	298.00	120.00
23	Water	21.00	374.24	110.00
24	Air	15.00	298.00	110.00
25	Air	15.00	766.40	2200.00
26	Slurry	40.64	298.00	110.00
27	Slurry	40.64	298.01	2200.00
28	Gas	48.20	930.02	2200.00

[a]After cleaning to set alkaline concentration within acceptable levels. [b]Liquid water. [c]After cleaning to set particle size and content within acceptable levels.

Table 8. *Power Input and Output of each Equipment of the Process*

Equipment #	Equipment Type	Power (Input/Output)	Power (MW)
1	Compressor	Input	102.72
3	Gas Turbine	Output	207.16
5	Steam Turbine	Output	61.98
7	Pump	Input	< 0.01
8	Pump	Input	0.63
10	Compressor	Input	29.76
12	Steam Turbine	Output	2.63
14	Pump	Input	0.04
15	Pump	Input	< 0.01
16	Compressor	Input	7.38
17	Pump	Input	0.08

Table 9. *Overall Efficiency Data of the Proposed Process*

Parameter	Value
mechanical power input[a] (MW)	140.62
mechanical power output[b] (MW)	271.76
net mechanical power output (MW)	131.15
efficiency based on 1st Law[c] (%)	40.27
efficiency based on 2nd Law[d] (%)	40.09

[a]Due to compressors and pumps. [b]From steam and gas turbines. [c]Defined as follows: (useful mechanical power output)/(rate of energy inputted by fuel). [d]Defined as follows: (useful mechanical power output)/(rate of exergy inputted by fuel).

Finally, Figure 19 shows the process 1st and 2nd Law efficiencies for different values of solid content in the MSW slurry, regarding the dryer bed diameter of 3.0 m.

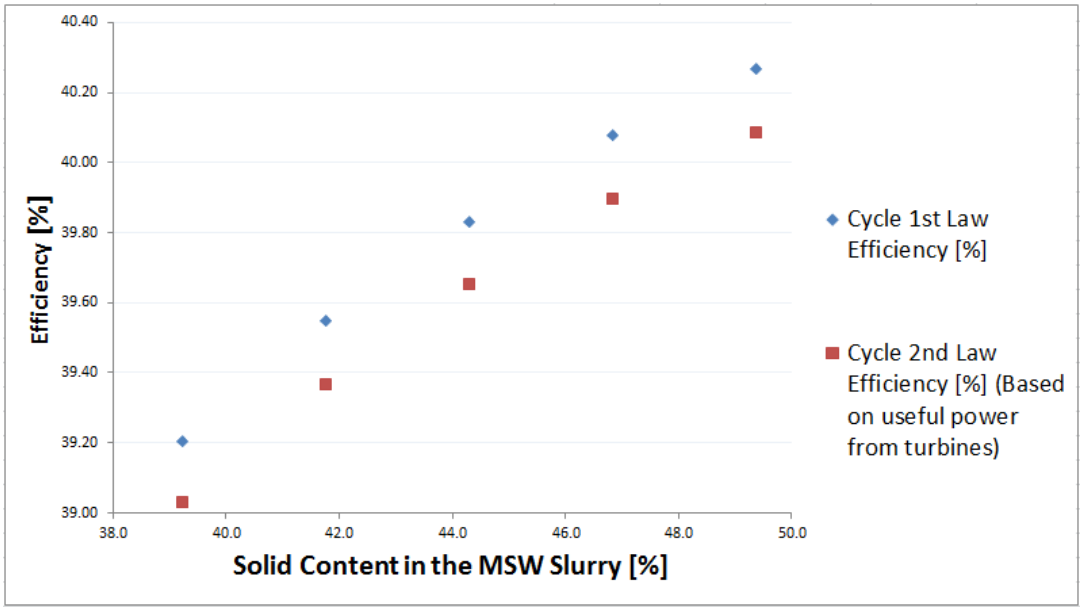

Figure 19. *Process 1st and 2nd Law efficiencies against solid content in the MSW slurry*

As seen, the efficiency increases with the increase of dry solid content in the slurry. This result was expected, but limitations on that content should be observed to allow feasible operations of commercial slurry pumps.

The overall efficiency value is relatively high when compared with the present 20% level, usually achieved by Rankine cycles in operation at sugar mills. That efficiency value was informed by a large boiler manufacturer engineering team [56] even if all steam would be diverted to power generation. The efficiency estimated here is also higher than the 33% achieved in studies aiming the application of BIG/GT process consuming bagasse [29].

8 CONCLUSIONS

The present work studied the influence of water content in MSW-water slurries consumed by the FSIG/GT thermoelectric power generation process. The results showed that the overall exergy efficiency of the process is inversely proportional to the amount of water added to the slurry. The lower limit for that water content is the minimum that would allow a slurry to be pumped using commercial equipment [51].

Despite of the low heating value of the MSW, it was possible to show that the power generation process 1st Law efficiency could reach 40.27%. That value is higher than the 34.78% obtained in a previous work [42] and well above the 20% level, as informed by a large boiler manufacturer engineering team [56] even if all steam would be diverted to power generation. The efficiency estimated here is also higher than the 33% achieved in studies aiming the application of BIG/GT process consuming bagasse [29].

Among many aspects, future works should:

a) Perform economic studies to assess the financial viability of the proposed alternative;
b) Evaluate the limits for solids content in the fuel slurry to allow pumping using commercially available equipment. That must require experimental investigations;
c) Revisit many parameters and conditions assumed here. For instance, dryer and gasifier operations with higher pressures. The FSIG/GT configuration may be also modified. Those would probably lead to increases in the process efficiency.
d) A review on the assumed parameters would be required. For instance, the maximum temperature around 900 K for steam turbine injections has been reported [82-84]. Improvements in the Rankine cycles are also possible, as for instance discharging from turbines of streams with steam quality near 90% are also possible. Despite changing some of the results presented here, it is believed that such would not invalidate or deeply change the findings of the work.

REFERENCES

1. Resenha Energética Brasileira - Edição de Maio de 2016, available at http://www.mme.gov.br/documents/10584/3580498/02+-+Resenha+Energ%C3%A9tica+Bra sileira+2016+-+Ano+Base+2015+(PDF)/66e011ce-f34b-419e-adf1-8a3853c95fd4;jsessionid =B415252F7145EC1BD6596B2C8137D1B8.srv155?version=1.0 (accessed Nov 21, 2016).

2. Brazilian Energy Balance - year 2015, available at https://ben.epe.gov.br/downloads/ Relatorio_Final_BEN_2016.pdf (accessed Nov 21, 2016).

3. Plano Decenal de Expansão de Energia 2024, available at http://www.epe.gov.br/PDEE/ Relat%C3%B3rio%20Final%20do%20PDE%202024.pdf (accessed Nov 21, 2016).

4. Apenas 3% de Todo o Lixo Produzido no Brasil é Reciclado, available at g1.globo.com/jornal-hoje/noticia/2015/04/apenas-3-de-todo-o-lixo-produzido-no-brasil-e-reciclado.html (accessed May 18, 2017).

5. Paro, A. C.; Costa, F. C.; Coelho, S. T. Estudo Comparativo para o Tratamento de Resíduos Sólidos Urbanos: Aterros Sanitários x Incineração. Revista Brasileira de Energia, 2008, 14 #2, 113-125.

6. Scandrett, L. A. Clift, R. The Thermodynamics of Alkali Removal from Coal-Derived Gases. Journal of the Institute of Energy, 57, 391-97. ISSN : 0144-2600 CODEN : JINEDX (1984).

7. Spacil, H. S. Luthura, K. L. Volatilization/Condensation of Alkali Salts in a Pressurized Fluidized Bed Coal Combustor/Gas Turbine Combined Cycle. Journal of the Electrochem. Soc., 129(9), 2119-2126 DOI.org/10.1149/1.2124391 (1982).

8. Oakey, J. Simms, N. Kilgallon, P. Gas turbines: gas cleaning requirements for biomass-fired systems. Materials Research, 7(1), 17-25 DOI.org/10.1590/S1516-14392004000100004 (2004).

9. Cheng, H.; Zhang, Y.; Meng, A.; Li, Q. Municipal Solid Waste Fueled Power Generation in China: A Case Study of Waste-to-Energy in Changchun City. Environ. Sci. Technol. [Online] 2007, 41(21), 7509−7515. http://pubs.acs.org/doi/abs/10.1021/es071416g (accessed Nov 28, 2016).

10. Akkaya, E.; Demir, A. Energy Content Estimation of Municipal Solid Waste by Multiple Regression Analysis. Presented at 5th International Advanced Technologies Symposium (IATS'09), Karabuk, Turkey, May 13−15, 2009. http://iats09.karabuk.edu.tr/press/bildiriler_pdf/IATS09_03-99_1292.pdf (accessed Nov 28, 2016).

11. The Conference Board of Canada. Municipal Waste Generation. http://www.conferenceboard.ca/hcp/Details/Environment/municipal-waste-generation.aspx (accessed Nov 28, 2016).

12. Smith, A.; Brown, K.; Ogilvie, S.; Rushton, K.; Bates, J. Waste Management Options and Climate Change. European Commission, DG Environment, July 2001.

13. Ryu, C. Potential of Municipal Solid Waste for Renewable Energy Production and Reduction of Greenhouse Gas Emissions in South Korea. J. Air Waste Manage. Assoc. [Online] 2012, 60, 173−183. http://www.tandfonline.com/doi/abs/10.3155/1047-3289.60.2.176#.UikS99K-r3s (accessed Nov 28, 2016).

14. Panorama dos Resíduos Sólidos no Brasil - 2015, available at http://www.abrelpe.org.br/Panorama/panorama2015.pdf (accessed Nov 12, 2017).

15. Helou, A. E.; Tran, K.; Buncio, C. Energy Recovery from Municipal Solid Waste in California: Needs and Challenges, Proceeding of the 18th Annual North American Waste-to-Energy Conference, Orlando, FL, May 11−13, 2010.

16. Domalski, E. S.; Jobe, T. L., Jr.; Milne, T. A. Thermodynamic Data for Biomass Conversion and Waste Incineration, 1986. National Bureau of Standards and Solar Energy Research Institute. http://www.nrel.gov/biomass/pdfs/2839.pdf (accessed Nov 28, 2016).

17. Gidarakos, E.; Havas, G.; Ntzamilis, P. Municipal Solid Waste Composition Determination Supporting the Integrated Solid Waste Management System in the Island of Crete. Waste Manage. [Online] 2006, 26(6), 668−679. http://www.seas.columbia.edu/earth/wtert/sofos/Gidarakos_Counrty%20report.pdf (accessed Nov 28, 2016).

18. Cant, M. Municipal Solid Waste (MSW) Options: Integrating Organics Management and Residual Treatment/Disposal. Municipal Waste Integration Network and Recycling Council of Alberta, April 2006.

19. Kautto, N.; Waldau, A. J. Renewable Energy Snapshots 2009. European Commission and Institute for Energy, March 2009.

20. Paleologos, E. K.; Economopoulos, A. P.; Rambow, B. Waste-to-Energy Alternatives: An Overview of Technologies, Regulatory Framework, and Economics, Haz. Waste Management, October 2008.

21. Anthony, E. J. Fluidized Bed Combustion of Alternative Solid Fuels; Status, Successes and Problems of the Technology. Prog. Energy Combust. Sci. 1995, 21, 239−268.

22. Williams, R. H. Biomass Gasifier/Gas Turbine Power and Greenhouse Warming. IEA/OECD Expert Seminar on Energy Technologies for Reducing Emissions of Greenhouse Gases, Paris, France, April 12−14, 1989.

23. Ogden, J. M.; Williams, R. H.; Fulmer, M. E. Cogeneration Applications of Biomass Gasifier/Gas Turbine Technologies in the Cane Sugar and Alcohol Industries. Conference on Energy and Environment in the 21st Century, Cambridge, MA, March 26−28, 1990.

24. Larson, E. D. Biomass-Gasifier/Gas-Turbine Cogeneration in the Pulp and Paper Industry. 36th ASME International Gas Turbine and Aeroengine Congress and Exhibition, Orlando, FL, June 3−6, 1991.

25. Larson, E. D.; Marrison, C. I. Economic Scales for First-Generation Biomass-Gasifier/Gas Turbine Combined Cycles Fueled from Energy Plantations. Turbo Expo' 96, the 41st ASME Gas Turbine and Aeroderivative Congress, Birmingham, England, June 10−13, 1996.

26. Larson, E. D.; Hughes, W. E. M. Performance Modeling of Aeroderivative Steam-Injected Gas Turbines and Combined Cycles Fueled from Fixed or Fluid-Bed Biomass Gasifiers. Turbo Expo'96, the 41st ASME Gas Turbine and Aeroengine Congress, Birmingham, England, June 10−13, 1996.

27. Consonni, S.; Larson, E. D. Biomass-Gasifier/Aeroderivative Gas Turbine Combined Cycles; Part A: Technologies and Performance Modeling. Cogen Turbo Power'94, The American Society of Mechanical Engineers' 8th Congress & Exposition on Gas Turbines in Cogeneration and Utility, Industrial and Independent Power Generation, Portland, OR, October 25−27, 1994.

28. Consonni, S.; Larson, E. D. Biomass-Gasifier/Aeroderivative Gas Turbine Combined Cycles; Part B: Performance Calculations and Economic Assessment. Cogen Turbo Power'94, The American Society of Mechanical Engineers' 8th Congress & Exposition on Gas Turbines in Cogeneration and Utility, Industrial and Independent Power Generation, Portland, OR, October 25−27, 1994.

29. Larson, E. D.; Williams, R. H.; Leal, M. R. L. V. A Review of Biomass Integrated-Gasifier/Gas Turbine Combined Cycle Technology and Its Application in Sugarcane Industries, with an Analysis for Cuba. Energy Sustainable Dev. [Online] 2001, 5(1), 54−76 http://www.sciencedirect.com/science/article/pii/S0973082609600211 (accessed Nov 28, 2016).

30. Lehtovaara, A.; Mojtahedi, W. Ceramic-Filter Behavior in Gasification. Bioresour. Technol. 1993, 46, 113−118.

31. Pedersen, K.; Malmgreem-Hansen, B.; Petersen, P. Catalytic Cleaning of Hot Gas Filtration. Biomass for Energy and the Environment. Proceedings of 9th European Bioenergy Conference, Copenhagen, Denmark, June 24−27, 1996; Chartier, P., Ferrero, G. L., Henius, U. M., Hultberg, S., Sachau, J., Wiinbland, M., Eds.; Pergamon Press: 1996; pp 1312−1317.

32. Horner, M. W. Simplified IGCC with Hot Fuel Gas Combustion (85-JPGC-GT-13). ASME/IEEE Power Generation Conference, Milwaukee, WI, 1985.

33. Scandrett, L. A.; Clift, R. The Thermodynamics of Alkali Removal from Coal-Derived Gases. J. Institute Energy 1984, 57, 391−97.

34. Spacil, H. S.; Luthura, K. L. Volatilization/Condensation of Alkali Salts in a Pressurized Fluidized Bed Coal Combustor/Gas Turbine Combined Cycle. J. Electrochem. Soc. 1982, 129 (9), 2119−2126.

35. Oakey, J.; Simms, N.; Kilgallon, P. Gas Turbines: Gas Cleaning Requirements for Biomass-Fired Systems. Mater. Res. 2004, 7 (1), 17-25.

36. US PATENT NUMBER 20110146153, High Pressure Feeder and Method of Operating to Feed Granular or Fine Materials , available at www.google.com/patents/US20110146153 (accessed Nov 24, 2013).

37. Dai, J.; Cui, H.; Grace, J. R. Biomass feeding for thermochemical reactors. Progress in Energy and Combustion Science [Online] 2012, 38 (5), 716-736. https://doi.org/10.1016/j.pecs.2012.04.002. (accessed Oct 07, 2017).

38. de Souza-Santos, M. L.; Chavez, J. V. Preliminary Studies on Advanced Power Generation Based on Combined Cycle Using a Single High-Pressure Fluidized Bed Boiler and Consuming Sugar-Cane Bagasse. Fuel [Online] 2012, 95, 221−225. http://dx.doi.org/10.1016/j.fuel.2011.12.008 (accessed Nov 28, 2016).

39. de Souza-Santos M. L.; Chavez J. V. Development of Studies on Advanced Power Generation Based on Combined Cycle Using a Single High-Pressure Fluidized Bed Boiler and Consuming Sugar Cane Bagasse. Energy Fuels [Online] 2012, 26, 1952−1963. http://dx.doi.org/10.1021/ef2019935 (accessed Nov 28, 2016).

40. de Souza-Santos, M. L.; Chavez, J. V. Second Round on Advanced Power Generation Based on Combined Cycle Using a Single High-Pressure Fluidized Bed Boiler and Consuming Biomass. Open Chem. Eng. J. [Online] 2012, 6, 41−4. http://benthamopen.com/contents/pdf/TOCENGJ/TOCENGJ-6-41.pdf (accessed Nov 28, 2016).

41. de Souza-Santos, M. L.; Ceribeli K. Technical Evaluation of a Power Generation Process Consuming Municipal Solid Waste. Fuel [Online] 2012, 108, 578−585. http://www.sciencedirect.com/science/article/pii/S0016236112010617 (accessed Nov 28, 2016).

42. de Souza-Santos, M. L.; Ceribeli K. Fuel-Slurry Integrated Gasifier/Gas Turbine (FSIG/GT) Alternative for Power Generation Applied to Municipal Solid Waste (MSW). Energy Fuels [Online] 2013, 27, 7696−7713. http://dx.doi.org/10.1021/ef401878v (accessed Nov 21, 2016).

43. The Gasification Process, available at http://www.gasification-syngas.org/technology/the-gasification-process/ (accessed Dec 06, 2016).

44. Moran, M. J.; Shapiro, H. N.; Boettner, D. D.; Bailey, M. B. Fundamentals of Engineering Thermodynamics, 7th Edition. John Wiley & Sons, Inc. (2010).

45. Breault, R. W. Gasification Processes Old and New: A Basic Review of the Major Technologies. Energies [Online] 2010, 3, 216-240. http://dx.doi.org/ 10.3390/en3020216 (accessed Dec 13, 2016).

46. Lombardi, L. Carnevale, E. Corti, A. A review of technologies and performances of thermal treatment systems for energy recovery from waste. Waste Management [Online] 2015, 37, 26-44. http://dx.doi.org/10.1016/j.wasman.2014.11.010 (accessed Jan 10, 2017).

47. Babcock and Wilcox. SO2 Absorption in fluidized bed combustor of coal - effect of limestone particle size. Report EPRI FP-667, Project 719-1 (1978).

48. Basu, P. Combustion and gasification in fluidized beds. Boca Raton (FL): CRC Press (2006).

49. de Souza-Santos, M. L. Solid fuels combustion and gasification: modeling,simulation, and equipment operation, 2nd edition. New York: CRC Press (2010).

50. de Souza-Santos, M. L. Modelling and simulation of fluidized-bed boilers and gasifiers for carbonaceous solids, Ph.D. Dissertation. England, United Kingdom: University of Sheffield, Department of Chemical Engineer and Fuel Technology (1987).

51. He, W. Park, C. S. Norbeck, J. N. A Rheological Study on the Pumpability of Co-Mingled Biomass and Coal Slurries. International Pittsburgh Coal Conference 2008, Pittsburgh, PA, 2009, available at www.docin.com/p-46581930.html (accessed Mar 03, 2014).

52. Gresh, M. T. Sassos M. J. Watson A. Axial Air Compressors - Maintaining Peak Efficiency. turbolab.tamu.edu/proc/turboproc/T21/T21173-181.pdf (accessed Mar 03, 2014).

53. Boyce, P. M. Axial Flow Compressors. http://www.netl.doe.gov/File%20Library/Research/Coal/energy%20systems/turbines/handbook/2-0.pdf (accessed Aug 25, 2015).

54. Veres, J. P. Centrifugal and Axial Pump Design and Off-Design Performance Prediction. NASA Technical Memorandum 106745. www.grc.nasa.gov/WWW/RTT/docs/Veres_1994.pdf (accessed Mar 03, 2014).

55. Sommers, A. Wang, Q. Han, X. T'Joen, C. Park, Y. Jacobi, A. Ceramics and ceramic matrix composites for heat exchanges in advanced thermal systems - A review, Applied Thermal Engineering 2010, 30, 1277-1291.

56. Personal communication between Prof. de Souza-Santos and engineering staff of Dedini Industries. www.dedini.com.br/index.php?lang=en (accessed Mar 03, 2014).

57. de Souza-Santos, M. L. Proposals for power generation based on processes consuming biomass-glycerol slurries, Energy 2016, 1-16.

58. Sit, S. P. Grace, J. R. Effect of Bubble Interaction on the Interphase Mass Transfer in Gas Fluidised Beds. Chem. Engineering Science 1981, 36, 327-335.

59. La Nause, R. D. Jung, K. Kastl, J. Mass Transfer to Large Particles in Fluidised Beds of Small Particles. Chem. Engineering Science 1984, 39, 1623-1633.

60. Kunii, D. Levenspiel, O. Fluidization Engineering, 2nd edition. New York: John Wiley (1991).

61. Horio, M. Nonaka, A. A Generalized Bubble Diameter Correlation for Gas-Solid Fluidised Beds. AIChE Journal 1987, 33(11), 1865-1872.

62. Rabi, J. A. de Souza-Santos M. L. Incorporation of a two-flux model for radiative heat transfer in a comprehensive fluidized bed simulator. Part I: Preliminary theoretical investigations. Thermal Engineering 2003, 3, 64-70. ojs.c3sl.ufpr.br/ojs2/index.php/reterm/article/view/3516 (accessed Feb 24, 2017).

63. Rabi, J. A. de Souza-Santos M. L. Incorporation of a two-flux model for radiative heat transfer in a comprehensive fluidized bed simulator. Part II: Numerical results and assessment. Thermal Engineering 2004, 4, 49-54. ojs.c3sl.ufpr.br/ojs/index.php/reterm/article/view/3476 (accessed Feb 24, 2017).

64. de Souza-Santos, M. L. A New Version of CSFB, Comprehensive Simulator for Fluidized Bed Equipment. Fuel 2007, 86, 1684-1709. dx.doi.org/10.1016/j.fuel.2006.12.001 .

65. Rabi, J. A. de Souza-Santos, M. L. Comparison of Two Model Approaches Implemented in a Comprehensive Fluidized-Bed Simulator to Predict Radiative Heat Transfer: Results for a Coal-Fed Boiler. Computer and Experimental Simulations in Engineering and Science 2008, 3, 87-105.

66. de Souza-Santos, M. L. Comprehensive Modelling and Simulation of Fluidized-Bed Boilers and Gasifiers. Fuel 1989, 68, 1507-1521. doi.org/10.1016/0016-2361(89)90288-3.

67. Delvosalle, C. Vanderschuren, J. Gas-to-particles and Particle-to-particle Heat Transfer in Fluidised Beds of Large Particles. Chem. Engineering Science 1985, 40(5), 769-779.

68. Xavier, A. M. Davidson, J. F. In: Fluidization, eds. Davidson, J. F. and Keamis, D. L. Cambridge: Cambridge University Press (1978), pp 333.

69. Reid, C. R. Prausnitz, J. M. Poling, B. E. The Properties of Gases and Liquids, 4th. Edition. New York: McGraw-Hill (1987).

70. Karapetyants, M. K. Chemical Thermodynamics. Moscow: Mir (1978).

71. Soo, S. L. Note on Motions of Phases in a Fluidised Bed. Power Technology 1986, 45, 169-172.

72. Soo, S. L. Average Circulatory Motion of Particles in Fluidised Beds, Power Technology 1989, 57, 107 117.

73. Soo, S. L. Particulates and Continuum, Multiphase Fluid Dynamics. New York: Hemisphere (1989).

74. Costa, M. A. S. de Souza-Santos, M, L. Studies on the Mathematical Modeling of Circulation Rate of Particles in Bubbling Fluidized Beds. Powder Technology 1999, 103, 110-116. doi.org/10.1016/S0032-5910(98)00227-7.

75. Wen, C. Y. Chen, L. H. Fluidised Bed Freeboard Phenomena: Entrainment and Elutriation. AIChE Journal 1982, 28, 117.

76. Niksa, S. Kerstein, A. R. On the role of macromolecular configuration in rapid coal devolatilization. Fuel 1987, 66, 1389-1399.

77. Niksa, S. Rapid coal devolatilization as an equilibrium flash distillation. AIChE Journal 1988, 34, 790-802.

78. Solomon, P. R. Colket, M. B. Seventeenth Symposium (International) on Combustion. The Combustion Institute, Pittsburgh, PA, 1979, pp 131.

79. Solomon, P. R. Serio, M. A. Carangelo RM, Markham JR. Very rapid coal pyrolysis. Fuel 1986, 65, 182-193.

80. Serio, M. A. Hamblen, D. G. Markham, J. R. Solomon, P. R. Kinetics of volatile evolution in coal pyrolysis: experiment and theory. Energy & Fuels 1987, 1, 138-152.

81. Solomon, P. R. Hamblen, D. G. Carangelo, R. M. Serio, M. A. Deshpande, G. V. General model of coal devolatilization. Energy & Fuels 1988, 2, 405-422.

82. SIEMENS. Siemens Steam Turbine SST-400. Available at: <https://www.energy.siemens.com/hq/en/fossil-power-generation/steam-turbines/sst-400.htm#content=Technical%20Data> (accessed Jun 21, 2017).

83. SIEMENS. Siemens Steam Turbine SST-700/900. Available at: <https://www.energy.siemens.com/hq/en/fossil-power-generation/steam-turbines/sst-700-900.htm> (accessed Jun 21, 2017).

84. SIEMENS. Siemens Steam Turbine SST-6000. Available at: <https://www.energy.siemens.com/hq/en/fossil-power-generation/steam-turbines/sst-6000.htm#content=Technical%20Data> (accessed Jun 21, 2017).

APPENDIX 1 - COMPREHENSIVE SIMULATOR OF FLUIDIZED AND MOVING BED EQUIPMENT (CESFAMB©) MOST RELEVANT EQUATIONS

The most important relationships of the model are listed below [49, 57].

- Mass balance in the emulsion gas:

$$\frac{dF_{GE,j}}{dz} = \sum_{m=1}^{3}\left(R_{het,SE,m,j}\gamma_{m,E}S_E\right) + R_{hom,GE,j}\varepsilon_E S_E + G_{MGEGB,j}\gamma_B S \quad , \qquad 1 \le j. \le 500 \tag{A.1}$$

j smaller than 501 refers to gaseous components while equal or above 500 to solid phase ones.

- Mass balance in the bubble phase:

$$\frac{dF_{GB,j}}{dz} = R_{hom,GB,j}\varepsilon_B S - G_{MGEGB,j}\gamma_B S \quad , \qquad 1 \le j \le 500 \tag{A.2}$$

- Conversion of solids in the bed section:

$$\Lambda_{D,j} = 1 - \frac{F_{LD,j}}{F_{ID,j}} \quad , \quad 501 \le j \le 1000 \tag{A.3}$$

where, due to simplification “F”, the mass flow ($F_{LD,j}$) of component “j” leaving the bed is given by an average computed throughout the entire bed, or

$$F_{LD,j} = F_{ID,j} - \sum_{m=1}^{3}\int_{z=0}^{z_D} R_{het,SE,m,j}\gamma_{m,E}S_E \, dz \quad , 501 \le j \le 1000 \tag{A.4}$$

- Energy balance for the emulsion gas:

$$F_{GE}c_{GE}\frac{dT_{GE}}{dz} = \varepsilon_E S_E\left[-R_{QGE} + \sum_{m=1}^{3}(R_{CSEGE,m} + R_{hSEGE,m}) + \left(R_{CGBGE} + R_{MGBGE}\right)\frac{\varepsilon_B}{\varepsilon_E} - R_{CGETD} - R_{GEWD}\right] \tag{A.5}$$

where

$$F_{GE} = \sum_{j=1}^{500} F_{GE,j} \tag{A.6}$$

- Energy balance for the bubble phase:

$$F_{GB}c_{GB}\frac{dT_{GB}}{dz}=\varepsilon_B S\left[-R_{QGB}-R_{CGBGE}-R_{hGBGE}-R_{CGBTD}\right] \tag{A.7}$$

where

$$F_{GB}=\sum_{j=1}^{500}F_{GB,j} \tag{A.8}$$

- Energy balances for solid phases in the bed:

$$F_{H,m}c_{SE,m}\frac{dT_{SE}}{dz}=\gamma_{m,E}S_E\left[-R_{QSE,m}-\left(R_{CSEGE,m}+R_{hSEGE,m}\right)\frac{\varepsilon_E}{1-\varepsilon_E}\right.$$
$$\left.-R_{RSETD,m}-\sum_{n=1}^{3}\left(R_{RSESE,m,n}+R_{CSESE,m,n}\right)\right] \quad , 1\le m\le 3 \tag{A.9}$$

where "m" indicates the solid phase (1 = carbonaceous; 2 = limestone or any sulphur absorbent; 3 = inert) present in the bed.

- Mass balances for the components in the freeboard:

$$\frac{dF_{F,j}}{dz}=\sum_{m=1}^{3}\left(R_{het,SF,m,j}\frac{dA_{PF,m}}{dz}\right)+R_{hom,GF,j}\frac{dV_{GF}}{dz} \quad , \quad 1\le j\le 1000 \tag{A.10}$$

- Energy balances for gases in the freeboard:

$$F_{GF}c_{GF}\frac{dT_{GF}}{dz}=\frac{dV_{GF}}{dz}\left[-R_{QGF}\right.$$
$$\left.+\sum_{m=1}^{3}\left(R_{CSFGF,m}+R_{hSFGF,m}\right)-R_{CGFTF}-R_{GFWF}\right] \tag{A.11}$$

where

$$F_{GF}=\sum_{j=1}^{500}F_{F,j} \tag{A.12}$$

- Energy balances for the solids in the freeboard:

$$F_{SF,m}c_{SF,m}\frac{dT_{SF,m}}{dz}=\frac{dV_{SF,m}}{dz}\left[-R_{QSF,m}-\left(R_{CSFGF,m}+R_{hSFGF,m}\right)\frac{dV_{GF}/dz}{dV_{SF,m}/dz}\right.$$
$$\left.-R_{RSFTF,m}-\sum_{n=1}^{3}\left(R_{RSFSF,m,n}\right)\right] \quad ,1\le m\le 3 \tag{A.13}$$

where

$$F_{SF,m} = \sum_{j=m\ comp.} F_{F,j} \tag{A.14}$$

- Mass flux of each chemical species "j" between bubbles and emulsion:

$$G_{MGEGB,j} = \psi_{BE}\tilde{\rho}_G M_j\left(x_{GB,j} - x_{GE,j}\right)\frac{A_B}{V_B} \tag{A.15}$$

where the mass transfer coefficient is calculated according to the work of Sit and Grace [58].

- Coefficient of mass transfer between phase formed by particles kind "m" and the emulsion gas:

$$\psi_{SEGE,m} = N_{Sh,m}\frac{D_G\tilde{\rho}_{GE}}{d_m} \tag{A.17}$$

where the Sherwood number is calculated according to the work of La Nause [59].

- Heat transfer between bubbles and emulsion:

$$R_{CGBGE} = \alpha_{CGBGE}(T_{GB} - T_{GE})\frac{dA_B}{dV_B} \tag{A.18}$$

where the coefficient is taken from the literature [60]. The ratio of bubble area and volume is a simple function of the bubble diameter [49]. However, that diameter varies throughout the bed according to Horio and Nokada correlations [61].

- Heat transfer by convection between the solid particle "m" and the gas in the emulsion:

$$R_{CSEGE,m} = \alpha_{CSEGE,m}(T_{SE,m} - T_{GE})\frac{dA_{PE,m}}{dV_{GE}} \tag{A.19}$$

where the method to compute the heat transfer coefficient can be found elsewhere [49].

- Radiative heat transfer between particles applies the two-flux method, as described elsewhere [62-65]. However, the results obtained with that approach does not improve too much on the simpler attack assuming grey bodies of the original work [50, 66], or:

$$R_{RSESE,m,n} = \frac{\sigma\left(T_{PE,m}^4 - T_{PE,n}^4\right)}{\frac{1-\varepsilon'_m}{\varepsilon'_m} + \frac{1-\varepsilon'_n}{\varepsilon'_n}\frac{f''_m}{f''_n} + \frac{1}{f''_n}}\frac{dA_{PE,m}}{dV_{SE,m}} \tag{A.20}$$

where the view factor between particles “m” and “n” given by their area fractions in the mixture of particles. Those values are obtained at each point through the solution of differential mass and energy balances plus routines related to fine particles generation (by attrition) and entrainment [49, 50].

- Heat transfer by convection between particles:

$$R_{CSESE,m,n} = \alpha_{SESE,m,n} f''_n \left(T_{PE,m} - T_{PE,n}\right) \frac{dA_{PE,m}/dz}{dV_{SE,m}/dz} \tag{A.21}$$

where the coefficient has been taken from the work by Delvosalle and Vanderschuren [67]. The ratio between the available area and volumes of particles “m” can be obtained from [49]:

$$\frac{dA_{PE,m}}{dz} = \frac{6}{d_m} f'''_m (1-\varepsilon_E)(1-\varepsilon_B)S \tag{A.22}$$

and

$$\frac{dV_{PE,m}}{dz} = f'''_m (1-\varepsilon_E)(1-\varepsilon_B)S \tag{A.23}$$

- Heat transfer by convection between emulsion interstitial gas and tubes (eventually present in the bed):

$$R_{CGETD} = \alpha_{EOTD}(T_{GE} - T_{WOTD}) \frac{dA_{OTD}/dz}{dV_{GE}/dz} \tag{A.24}$$

and the equivalent for the gas in the bubbles by

$$R_{CGBTD} = \alpha_{BOTD}(T_{GB} - T_{WOTD}) \frac{dA_{OTD}/dz}{dV_{GB}/dz} \tag{A.25}$$

The heat transfer coefficients are taken from Xavier and Davidson [68]. The available volumes of emulsion and bubbles at each slice “dz” of the bed is obtained from the relations already described combined with the differential mass and energy balances.

Properties of gases, liquids, and solids were taken from the literature [69, 70].

- Circulation rates of particles in the bed. As seen, the energy balances for solid phases in the bed (Eq. A.9) require the computation of overall rate of particles “m” in the axial direction ($F_{H,m}$). The new approach follows the works of Soo [71-73], which have been reviewed and adapted to the present model by Costa and de Souza Santos [74]. Accordingly, the following system of partial differential equations, representing the momentum transfers between the various phases in the bed, is set:

$$\left(\frac{1}{r}\right)\left[\frac{\partial\left(ru_{G,r}\right)}{\partial r}\right]+\left(\frac{\partial u_{G,z}}{\partial z}\right)=0 \tag{A.26}$$

$$\left(\frac{1}{r}\right)\left[\frac{\partial\left(ru_{p,r}\right)}{\partial r}\right]+\left(\frac{\partial u_{p,z}}{\partial z}\right)=0 \tag{A.27}$$

$$0=\rho_p\alpha_p\left(u_{G,z}-u_{p,z}\right)+\mu_p\left[\frac{1}{r}\frac{\partial}{\partial r}\left(r\frac{\partial u_{p,z}}{\partial r}\right)+\frac{\partial^2 u_{p,z}}{\partial z^2}\right]-\rho_p g \tag{A.28}$$

$$0=-\frac{\partial P}{\partial z}-\rho_p\alpha_p u_{G,z,z=0}-(\rho_p+\rho_G)g \tag{A.29}$$

and solve after proper boundary conditions [49, 74]. Thus, variables involving radial coordinate are introduced. Such an approach is one among the improvements made in the previous versions and provided a more reliable and precise simulation results.

The auxiliary relations in the freeboard are somewhat similar to the ones applied for the emulsion phase and are detailed elsewhere [49]. However, the equations related to dynamics are very different, and the most important ones are listed below.

- Entrainment rate [75]:

$$F_{Y,m,l}=F_{X,m,l}+(F_{Y,m,l,z=z_D}-F_{X,m,l})\exp[-a_Y(z-z_D)] \tag{A.30}$$

- The rate of elutriation is given by [75]:

$$F_{X,m,l}=w_{m,l}\rho_m(1-\varepsilon_{F,m,l})\left(U_G-u_{T,m,l}\right)S \tag{A.31}$$

- The entrainment rate at the top of the bed is provided by [75]:

$$F_{Y,m,l,z=z_D}=3.07x10^{-9}S^2 d_{B,z=z_D}\rho_G^{3.5}g^{0.5}\frac{\left(U_G-U_{G,mf}\right)^{2.5}_{z=z_D}}{\mu_G^{2.5}}f_m w_{m,l} \tag{A.32}$$

The particle size distribution found in the bed during steady-state operation is computed from the distribution of feeding particles and the combination of the effects of chemical reactions, attrition between particles, entrainment and elutriation [49].

The following chemical reactions are considered:

$$CH_{a_H}O_{a_O}N_{a_N}S_{a_S}+\left(\frac{1}{2}+\frac{a_H}{4}-\frac{a_O}{2}+\frac{a_N}{2}+a_S\right)O_2\rightarrow CO$$

$$+\frac{a_H}{2}H_2O+a_N NO+a_S SO_2 \tag{R.1}$$

$$CH_{a_H}O_{a_O}N_{a_N}S_{a_S} + (1-a_O)H_2O \leftrightarrow \left(1+\frac{a_H}{2}-a_O-a_S\right)H_2 + CO$$

$$+\frac{a_N}{2}N_2 + a_S H_2S \quad \text{(R.2)}$$

$$CH_{a_H}O_{a_O}N_{a_N}S_{a_S} + CO_2 \leftrightarrow 2CO + a_O H_2O + \left(\frac{a_H}{2}-a_O-\frac{3a_N}{2}-a_S\right)H_2$$

$$+ a_N NH_3 + a_S H_2S \quad \text{(R.3)}$$

$$CH_{a_H}O_{a_O}N_{a_N}S_{a_S} + \left(2-\frac{a_H}{2}+a_O+\frac{3}{2}a_N+a_S\right)H_2 \leftrightarrow CH_4 + a_O H_2O$$

$$+ a_N NH_3 + a_S H_2S \quad \text{(R.4)}$$

$$CH_{a_H}O_{a_O}N_{a_N}S_{a_S} + (2-a_O)NO \leftrightarrow \left(\frac{a_H}{2}-a_S\right)H_2 + CO_2$$

$$+\left(1+\frac{a_N}{2}-\frac{a_O}{2}\right)N_2 + a_S H_2S \quad \text{(R.5)}$$

$$Fuel_{daf} \rightarrow Volatile + Char_1 \quad \text{(R.6)}$$

$$Volatile \rightarrow Gases + Tar \quad \text{(R.7)}$$

$$Wet-Carbonaceous-Solid \leftrightarrow Dry-Carbonaceous-Solid + H_2O \quad \text{(R.8)}$$

$$CH_{a_H}O_{a_O}N_{a_N}S_{a_S} + (2-a_O)NO \leftrightarrow \left(\frac{a_H}{2}-a_S\right)H_2 + 2CO$$

$$+\left(1+\frac{a_N}{2}-\frac{a_O}{2}\right)N_2 + a_S H_2S \quad \text{(R.9)}$$

$$CH_{a_H}O_{a_O}N_{a_N}S_{a_S} + (1-a_O)N_2O \leftrightarrow \left(\frac{a_H}{2}-a_S\right)H_2 + CO$$

$$+\left(1+\frac{a_N}{2}-a_O\right)N_2 + a_S H_2S \quad \text{(R.10)}$$

$$Tar \rightarrow Char_2 \quad \text{(R.11)}$$

$$CaCO_3 \Leftrightarrow CaO + CO_2 \quad \text{(R.12)}$$

$$2CaO + 2SO_2 + O_2 \Leftrightarrow 2CaSO_4 \quad \text{(R.13)}$$

$$Wet-Absorbent \leftrightarrow Dry-Absorbent + H_2O \quad \text{(R.14)}$$

$$CaO + H_2S \Leftrightarrow CaS + H_2O \quad \text{(R.15)}$$

$$Wet - Solid - Inert \leftrightarrow Dry - Solid - Inert + H_2O \quad \text{(R.16)}$$

$$MgCO_3 \Leftrightarrow MgO + CO_2 \quad \text{(R.17)}$$

$$2MgO + 2SO_2 + O_2 \Leftrightarrow 2MgSO_4 \quad \text{(R.18)}$$

$$MgO + H_2S \Leftrightarrow MgS + H_2O \quad \text{(R.19)}$$

$$CO + H_2O \Leftrightarrow CO_2 + H_2 \quad \text{(R.20)}$$

$$2CO + O_2 \Leftrightarrow 2CO_2 \quad \text{(R.21)}$$

$$2H_2 + O_2 \Leftrightarrow 2H_2O \quad \text{(R.22)}$$

$$CH_4 + 2O_2 \Leftrightarrow CO_2 + 2H_2O \quad \text{(R.23)}$$

$$2C_2H_6 + 7O_2 \Leftrightarrow 4CO_2 + 6H_2O \quad \text{(R.24)}$$

$$4NH_3 + 5O_2 \Leftrightarrow 4NO + 6H_2O \quad \text{(R.25)}$$

$$2H_2S + 3O_2 \Leftrightarrow 2SO_2 + 2H_2O \quad \text{(R.26)}$$

$$N_2 + O_2 \Leftrightarrow 2NO \quad \text{(R.27)}$$

$$C_{b_C}H_{b_H}O_{b_O}N_{b_N}S_{b_S} + \left(b_C + \frac{b_H}{4} - \frac{b_O}{2} + \frac{b_N}{2} + b_S\right)O_2 \rightarrow b_C CO_2 + b_S SO_2 + b_N NO + \frac{b_H}{2}H_2O \quad \text{(R.28)}$$

$$C_{b_C}H_{b_H}O_{b_O}N_{b_N}S_{b_S} \rightarrow \left(\frac{b_H}{2} - 2b_C + 2b_O - \frac{3}{2}b_N - b_S\right)H_2 + b_O CO + b_S H_2S + b_N NH_3 + (b_C - b_O)CH_4 \quad \text{(R.29)}$$

$$C_{b_C}H_{b_H}O_{b_O}N_{b_N}S_{b_S} + \left(2b_C - \frac{b_H}{2} - 2b_O + \frac{3}{2}b_N + b_S\right)H_2 \rightarrow b_O CO + b_S H_2S + b_N NH_3 + (b_C - b_O)CH_4 \quad \text{(R.30)}$$

$$C_2H_4 + 3O_2 \Leftrightarrow 2CO_2 + 2H_2O \quad \text{(R.31)}$$

$$2C_3H_6 + 9O_2 \Leftrightarrow 6CO_2 + 6H_2O \quad \text{(R.32)}$$

$$C_3H_8 + 5O_2 \Leftrightarrow 3CO_2 + 4H_2O \quad \text{(R.33)}$$

$$2C_6H_6 + 15O_2 \Leftrightarrow 12CO_2 + 6H_2O \quad \text{(R.34)}$$

$$4HCN + 3O_2 \Leftrightarrow 4CO + 2N_2O + 2H_2 \quad \text{(R.35)}$$

$$CH_4 + H_2O \Leftrightarrow CO + 3H_2 \quad \text{(R.36)}$$

$$C_2H_4 + 2H_2O \Leftrightarrow 2CO + 4H_2 \quad \text{(R.37)}$$

$$C_2H_6 + 2H_2O \Leftrightarrow 2CO + 5H_2 \quad \text{(R.38)}$$

$$C_3H_6 + 3H_2O \Leftrightarrow 3CO + 6H_2 \quad \text{(R.39)}$$

$$C_3H_8 + 3H_2O \Leftrightarrow 3CO + 7H_2 \quad \text{(R.40)}$$

$$C_6H_6 + 6H_2O \Leftrightarrow 6CO + 9H_2 \quad \text{(R.41)}$$

$$2NO_2 + 2NH_3 \Leftrightarrow 4NO + 3H_2 \quad \text{(R.42)}$$

$$2NO + 2NH_3 \Leftrightarrow 2N_2O + 3H_2 \quad \text{(R.43)}$$

$$3N_2O + 2NH_3 \Leftrightarrow 4N_2 + 3H_2O \quad \text{(R.44)}$$

$$NO_2 + 2H_2 \Leftrightarrow NO + H_2O \quad \text{(R.45)}$$

$$2NO + H_2 \Leftrightarrow N_2O + H_2O \quad \text{(R.46)}$$

$$N_2O + H_2 \Leftrightarrow N_2 + H_2O \quad \text{(R.47)}$$

$$NO_2 + CO \Leftrightarrow NO + CO_2 \quad \text{(R.48)}$$

$$2NO + CO \Leftrightarrow N_2O + CO_2 \quad \text{(R.49)}$$

$$N_2O + CO \Leftrightarrow N_2 + CO_2 \quad \text{(R.50)}$$

$$NH_3 + CO \Leftrightarrow HCN + H_2O \quad \text{(R.51)}$$

$$2N_2 + O_2 \Leftrightarrow 2N_2O \quad \text{(R.52)}$$

$$2N_2O + O_2 \Leftrightarrow 4NO \quad \text{(R.53)}$$

$$2NO + O_2 \Leftrightarrow 2NO_2 \quad \text{(R.54)}$$

The rates of heterogeneous (gas-solid) reactions are computed by two possible models: unreacted-core and exposed-core. Both take into account resistances due to mass transfer at the gas boundary layer around the reacting solid particle as well combinations of kinetics and mass transfer resistances at the reacting nucleus. Additionally, the unreacted-core considers the mass transfer resistance imposed by the ash (or already spent material) around the unreacted nucleus. However, the exposed-core model assumes that detaches from the nucleus leaving the core exposed to reacting gases. Therefore, this last model neglects the mass transfer resistance posed by ash layer. The unreacted model is also extended to cases of drying and devolatilization, where the spent layer is the dry or char around the drying or

pyrolysing nucleus, respectively. The equations to allow computations of heterogeneous reaction rates have been deduced elsewhere [49] and are listed below:

$$\tilde{r}_i = \frac{2}{d_{p,I}} \frac{\tilde{\rho}_{j,\infty} - \tilde{\rho}_{j,eq}}{\sum_{k=1}^{3} U_{U,k}} \tag{A.33}$$

where the three resistances are given by

$$U_{U,1} = \frac{1}{N_{Sh} D_{j,G}} \tag{A.34}$$

$$U_{U,2} = \frac{1-a}{a D_{j,A}} \tag{A.35}$$

$$U_{U,3} = \frac{1}{a D_{j,N} [a\Phi \coth(a\Phi) - 1]} \tag{A.36}$$

The ones describing the rate for the exposed-core model are:

$$\tilde{r}_i = \frac{2}{d_{p,I}} \frac{\tilde{\rho}_{j,\infty} - \tilde{\rho}_{j,eq}}{\sum_{k=1}^{3} U_{X,k}} \tag{A.37}$$

where the three resistance are given by

$$U_{X,1} = \frac{1}{N_{Sh} D_{j,G}} = U_{U,1} \tag{A.38}$$

$$U_{X,2} = 0 \tag{A.39}$$

$$U_{X,3} = \frac{a}{D_{j,N} [a\Phi \coth(a\Phi) - 1]} = a^2 U_{U,3} \tag{A.40}$$

In all above relations, the Thiele modulus is defined as

$$\Phi = r_A \left[\frac{k_i}{D_{j,N}} \right]^{1/2} \tag{A.41}$$

Equations A.33 to A.41 should be used for spherical or near-spherical particles. Equations for other forms such as plates and cylinders (or near those forms) can be found elsewhere [49]. The kinetics coefficients for the reactions considered here have been taken from the literature [49], while treatments for pyrolysis adapted from publications in the area [76-81].